Open access • Book Chapter • DOI:10.1007/978-3-319-75972-2_9

On the Constraints Formulation in the Nonsmooth Generalized-α Method

— **Source link** ↗

Olivier Bruls, Vincent Acary, Alberrto Cardona

Institutions: University of Liège, French Institute for Research in Computer Science and Automation, National University of the Littoral

Topics: Numerical stability, Unilateral contact, Discretization, Numerical analysis and Lagrange multiplier

Related papers:

- Unilateral Contact and Dry Friction in Finite Freedom Dynamics

- Numerical time integration methods for nonsmooth systems. Part I. Low relative degree and electrical networks applications Part II. Nonsmooth mechanical systems with impacts

- Toward higher order event-capturing schemes and adaptive time-step strategies for nonsmooth multibody systems

- Simultaneous enforcement of constraints at position and velocity levels in the nonsmooth generalized-α scheme

- Convergence of the generalized- α scheme for constrained mechanical systems

On the Constraints Formulation in the Nonsmooth Generalized-α Method

Olivier Brüls, Vincent Acary, Alberto Cardona

On the Constraints Formulation in the Nonsmooth Generalized-α Method

Olivier Brüls, Vincent Acary, and Alberto Cardona

Abstract The simulation of flexible multibody systems with unilateral contact conditions and impacts requires advanced numerical methods. The nonsmooth generalized-α method was developed in order to combine an accurate and second-order time discretization of the smoother part of the dynamics and a consistent but first-order time discretization of the impulsive contributions. Compared to the Moreau-Jean scheme, this approach improves the quality of the numerical solution especially for the representation of the vibrating response of flexible bodies. It entirely relies on the formal definition of a so-called smooth motion that captures a non-impulsive part of the total nonsmooth motion. This definition may account for some contributions of the bilateral constraints and/or of the active unilateral constraints at velocity or at acceleration level. This chapter shows that the formulation of the constraints strongly influences the numerical stability and the computational cost of the method. A strategy to enforce the bilateral and unilateral constraints simultaneously at position, velocity and acceleration levels is also established with a careful formulation of the activation criteria based on augmented Lagrange multipliers. In the special case of smooth systems, a comparison is made with more standard solvers for differential-algebraic equations. The properties of this method are demonstrated using illustrative numerical examples of smooth and nonsmooth mechanical systems.

Olivier Brüls
University of Liège, Allée de la Découverte 9, 4000 Liège, Belgium, e-mail: o.bruls@uliege.be

Vincent Acary
INRIA Rhône-Alpes, Grenoble, France, e-mail: vincent.acary@inria.fr

Alberto Cardona
CIMEC, Universidad Nacional del Litoral-CONICET, Santa Fe, Argentina, e-mail: acardona@unl.edu.ar

1 Introduction

This chapter addresses the numerical simulation of mechanical systems composed of rigid and flexible bodies interconnected by kinematic joints and subject to frictionless contact conditions. These models are intended to the analysis of the dynamic interactions between motion, impacts and vibrations in various industrial applications such as in automotive, wind turbines, and robotic systems. The kinematic joints impose restrictions on the relative motions of the bodies and are modelled as bilateral constraints whereas the non-penetration conditions at the contact points are modelled as unilateral constraints. These unilateral constraints may cause impact phenomena so that the dynamic response becomes nonsmooth involving velocity jumps and impulsive reaction forces.

In many practical situations, the nonsmooth behaviours are nevertheless localized in space and/or in time. After spatial and time discretization, this implies that velocity jumps and impulsive forces are only observed for a limited number of coordinates and/or during a limited number of time steps. Even though the correct description of these velocity jumps and impulsive forces are of the utmost importance for the global consistency of the simulation, the quality of the results within the smooth parts of the motion is also essential.

The most popular time-stepping methods for nonsmooth systems, such as the Moreau-Jean scheme [25, 27] or the Schatzman-Paoli scheme [29, 30], are robust with respect to the treatment of nonsmooth phenomena but they lead to rather poor first-order approximations of the smooth parts of the motion and to high levels of numerical dissipation, which is particularly penalizing for the accurate representation of vibration phenomena in flexible systems. Also, the constraints are imposed at velocity level so that a constraint drift generally appears at position level. Alternatively, event-driven techniques, which adapt their time steps to the impact instants, can be used in combination with a higher order scheme during the free flight phases [20]. However, their performance decreases if the frequency of impacts increases and they cannot be used if accumulation phenomena, involving an infinite series of impact in a finite time interval, are present. A more detailed description of numerical methods for the simulation of nonsmooth systems can be found in [2].

These observations motivated the recent developments of more sophisticated time-stepping algorithms for nonsmooth systems which involve improved approximations of the smoother parts of the motion [12, 14, 34, 35, 37]. Several authors [1, 12, 36] also investigated the development of algorithms which simultaneously enforce the bilateral and unilateral constraints at velocity and position levels, so that any drift-off phenomenon is avoided. In this chapter, we revisit the nonsmooth generalized-α method introduced in [12, 14]. It relies on a splitting of the motion into smooth (non-impulsive) and nonsmooth (impulsive) contributions. The smooth contributions are integrated using the second-order generalized-α method whereas the nonsmooth contributions are integrated using a first-order backward Euler scheme. This method leads to qualitatively better solutions than the Moreau-Jean method, both for rigid and flexible systems.

If the splitting of the dynamics into smooth and nonsmooth contributions leads to algorithms with improved performance, some freedom remains in the precise definition of the smooth motion especially regarding the contributions of the bilateral and unilateral constraints. This question has a significant influence on the numerical stability of the solution in the presence of impacts and velocity jumps. In [14], the smooth motion was defined as an unconstrained motion whereas the bilateral constraints at velocity level were imposed in [12]. Here, we propose a definition of the smooth motion which involves the bilateral constraints and the active unilateral constraints at acceleration level.

After a description of the equations of motion in Sect. 2 and of the nonsmooth generalized-α method in Sect. 3, the special case of a smooth mechanical system without impact is addressed in Sect. 4 and a comparison with more standard solvers for differential-algebraic equations (DAEs) which are commonly used for the analysis of smooth multibody systems is performed. We show that the proposed algorithm can be interpreted as an index-1 formulation which simultaneously enforces the constraints at position, velocity and acceleration levels. In Sect. 5, the behaviour of the algorithm in the smooth case is studied based on the numerical example of a pendulum modelled as a DAE. In this example, a post-impact numerical solution is also reproduced by considering disturbed initial conditions at the acceleration level. This analysis reveals the high robustness and stability of the proposed algorithm.

Three examples of nonsmooth dynamic systems are studied in Sect. 6: a bouncing rigid pendulum, a bouncing flexible pendulum and the horizontal impact of an elastic bar. These examples intend to reveal the good properties of the algorithm for systems with bilateral constraints, impacts, accumulation phenomena, flexible bodies, finite contact duration, dynamic activation and deactivation of unilateral constraints. Also, it is shown that the numerical damping of the generalized-α is no more necessary for the stabilization of the constraints but is only useful for the stabilization of the spurious high frequency modes resulting from the finite element discretization of flexible bodies. The conclusions of the study are finally summarized in Sect. 7.

2 Nonsmooth dynamics

2.1 Mechanical systems with unilateral constraints

Let us consider a mechanical system with bilateral and unilateral constraints. For example, the bilateral constraints may represent the restrictions imposed by a kinematic joint which connects two bodies of the system, whereas a unilateral constraint may represent a non-penetration condition when two bodies are in contact. In a first step, we assume that no impact occurs in the system but that detachment phenomena may occur during the motion. The equations of motion are then expressed as

$$\dot{\mathbf{q}} = \mathbf{v} \tag{1a}$$

$$\mathbf{M}(\mathbf{q})\,\dot{\mathbf{v}} - \mathbf{g}_{\mathbf{q}}^{T}(\mathbf{q})\,\boldsymbol{\lambda} = \mathbf{f}(\mathbf{q},\mathbf{v},t) \tag{1b}$$

$$\mathbf{g}^{\overline{\mathscr{U}}}(\mathbf{q}) = \mathbf{0} \tag{1c}$$

$$\mathbf{0} \le \mathbf{g}^{\mathscr{U}}(\mathbf{q}) \perp \boldsymbol{\lambda}^{\mathscr{U}} \ge \mathbf{0} \tag{1d}$$

where t is the time; $\mathbf{q}$ is the vector of coordinates, e.g., the nodal coordinates of a finite element mesh; $\mathbf{v}$ is the vector of velocities; $\mathbf{M}(\mathbf{q})$ is the mass matrix, $\mathbf{f}(\mathbf{q},\mathbf{v},t) = \mathbf{f}^{\text{ext}}(t) - \mathbf{f}^{\text{damp}}(\mathbf{q},\mathbf{v}) - \mathbf{f}^{\text{int}}(\mathbf{q})$ collects the external, damping and internal forces; $\mathbf{g}$ is the combined set of bilateral and unilateral constraints; $\mathbf{g}_{\mathbf{q}}(\mathbf{q})$ is the matrix of constraint gradients; $\boldsymbol{\lambda}$ is the vector of Lagrange multipliers which represents the unilateral and bilateral reaction forces; $\mathscr{U}$ is the set of indices of the unilateral constraints; $\overline{\mathscr{U}}$ is its complementarity set, i.e., the set of bilateral constraints; $\mathscr{T} = \mathscr{U} \cup \overline{\mathscr{U}}$ is the total set of constraints, and we have

$$\mathbf{g} = \begin{bmatrix} \mathbf{g}^{\mathscr{U}} \\ \mathbf{g}^{\overline{\mathscr{U}}} \end{bmatrix}, \qquad \boldsymbol{\lambda} = \begin{bmatrix} \boldsymbol{\lambda}^{\mathscr{U}} \\ \boldsymbol{\lambda}^{\overline{\mathscr{U}}} \end{bmatrix} \tag{2}$$

Equation (1d) takes the form of a complementarity condition. For one contact $j \in \mathscr{U}$, the function $g^{j}(\mathbf{q})$ represents the signed gap distance which can be obtained from the contact kinematics. The contact condition imposes $g^{j}(\mathbf{q})\lambda^{j} = 0$ with both $g^{j}(\mathbf{q})$ and λ^{j} being non-negative, i.e., we do not authorize penetration and the reaction force can only be compressive.

The equations of motion (1) can be solved by time integration from given initial conditions $\mathbf{q}(0) = \mathbf{q}_0$ and $\mathbf{v}(0) = \mathbf{v}_0$ in order to obtain the trajectory $\mathbf{q}(t)$, $\mathbf{v}(t)$ and the Lagrange multipliers $\boldsymbol{\lambda}(t)$ on a given time interval $[0,T]$. Though, the equations of motion also hide a purely algebraic relationship between $\mathbf{q}(t)$, $\mathbf{v}(t)$ and $\boldsymbol{\lambda}(t)$. Indeed, at a given time t, the constraint reaction forces $\boldsymbol{\lambda}(t)$ can be evaluated as an algebraic function of the current position $\mathbf{q}(t)$ and velocity $\mathbf{v}(t)$. As described below, the expression of this function is obtained by constraint differentiation.

If the bilateral constraints are satisfied at position level, then their first and second time-derivatives also vanish leading to the expression of the bilateral constraints at velocity level

$$\frac{\mathrm{d}\mathbf{g}(\mathbf{q}(t))}{\mathrm{d}t} = \mathbf{g}_{\mathbf{q}}^{\overline{U}}(\mathbf{q})\,\mathbf{v} = \mathbf{0} \tag{3}$$

and at acceleration level

$$\frac{\mathrm{d}^{2}\mathbf{g}(\mathbf{q}(t))}{\mathrm{d}t^{2}} = \mathbf{g}_{\mathbf{q}}^{\overline{U}}(\mathbf{q})\,\dot{\mathbf{v}} + \mathbf{h}^{\overline{U}}(\mathbf{q},\mathbf{v}) = \mathbf{0} \tag{4}$$

where $\mathbf{h}(\mathbf{q},\mathbf{v})$ is a quadratic operator with respect to its second argument. This operator is defined as

$$\mathbf{h}(\mathbf{q},\mathbf{v}) = \frac{\partial \mathbf{s}(\mathbf{q},\mathbf{v})}{\partial \mathbf{q}}\,\mathbf{v} \tag{5}$$

with $\mathbf{s}(\mathbf{q},\mathbf{v}) = \mathbf{g}_{\mathbf{q}}(\mathbf{q})\,\mathbf{v}$.

The unilateral constraint $j \in \mathcal{U}$ is active at position level at time t_i if $g^j(t_i) = 0$. As $\lambda^j \geq 0$, this constraint is such that $\lambda^j(t_i) - r g^j(t_i) \geq 0$ where $r > 0$ is a strictly positive yet arbitrary real number. The variable $\lambda^j(t) - r g^j(t)$ is an augmented Lagrange multiplier as encountered in augmented Lagrangian formulations [3, 31, 32]. The set of active unilateral constraints at position level is thus defined as

$$\mathcal{U}_A(t) = \{ j \in \mathcal{U} : \lambda^j(t) - r g^j(\mathbf{q}(t)) \geq 0 \} \tag{6}$$

In order to avoid penetration right after t_i, any constraint j in $\mathcal{U}_A(t_i)$ needs to be increasing so the gap velocity $\dot{g}^j = g_{\mathbf{q}}^j(\mathbf{q}(t_i)) \mathbf{v}(t_i)$ can only be non-negative. Hence, the unilateral constraint is transferred at velocity level as [33]

$$0 \leq g_{\mathbf{q}}^j(\mathbf{q}(t)) \mathbf{v}(t) \perp \lambda^j \geq 0, \quad \forall j \in \mathcal{U}_A(t) \tag{7}$$

The unilateral constraint $j \in \mathcal{U}$ is active at velocity level at time t_i if $g^j(\mathbf{q}(t_i)) = 0$ and $g_{\mathbf{q}}^j(\mathbf{q}(t_i)) \mathbf{v}(t_i) = 0$. As $\lambda^j \geq 0$, this constraint satisfies $\lambda^j(t_i) - r g_{\mathbf{q}}^j(\mathbf{q}(t_i)) \mathbf{v}(t_i) \geq 0$ for $r > 0$. The set of active unilateral constraints at velocity level is thus defined as

$$\mathcal{U}_B(t) = \{ j \in \mathcal{U}_A(t) : \lambda^j(t) - r g_{\mathbf{q}}^j(\mathbf{q}(t)) \mathbf{v}(t) \geq 0 \} \tag{8}$$

In order to avoid penetration right after t_i, the gap acceleration $\ddot{g}^j = g_{\mathbf{q}}^j(\mathbf{q}(t_i)) \dot{\mathbf{v}}(t_i) + h^j(\mathbf{q}(t_i), \mathbf{v}(t_i))$ needs to be non-negative for any constraint $j \in \mathcal{U}_B(t_i)$. The unilateral constraint is thus further transferred at acceleration level as [33]

$$0 \leq g_{\mathbf{q}}^j(\mathbf{q}(t)) \dot{\mathbf{v}}(t) + h^j(\mathbf{q}(t), \mathbf{v}(t)) \perp \lambda^j(t) \geq 0, \quad \forall j \in \mathcal{U}_B(t) \tag{9}$$

The unilateral constraint $j \in \mathcal{U}$ is active at acceleration level at time t_i if $g^j(\mathbf{q}(t_i)) = 0$, $g_{\mathbf{q}}^j(\mathbf{q}(t_i)) \mathbf{v}(t_i) = 0$ and $g_{\mathbf{q}}^j(\mathbf{q}(t_i)) \dot{\mathbf{v}}(t_i) + h^j(\mathbf{q}(t_i), \mathbf{v}(t_i)) = 0$. Following a similar argument as above, the set of active unilateral constraints at acceleration level is thus defined as

$$\mathcal{U}_C(t) = \{ j \in \mathcal{U}_B(t) : \lambda^j(t) - r(g_{\mathbf{q}}^j(\mathbf{q}(t)) \dot{\mathbf{v}}(t) + h^j(\mathbf{q}(t), \mathbf{v}(t))) \geq 0 \} \tag{10}$$

For convenience, we also introduce the active sets $\mathscr{A}(t) = \overline{\mathcal{U}} \cup \mathcal{U}_A(t)$, $\mathscr{B}(t) = \overline{\mathcal{U}} \cup \mathcal{U}_B(t)$, $\mathscr{C}(t) = \overline{\mathcal{U}} \cup \mathcal{U}_C(t)$ and the inactive sets $\overline{\mathscr{A}}(t) = \mathcal{T} \setminus \mathscr{A}(t)$, $\overline{\mathscr{B}}(t) = \mathcal{T} \setminus \mathscr{B}(t)$ and $\overline{\mathscr{C}}(t) = \mathcal{T} \setminus \mathscr{C}(t)$.

Using these definitions of the active sets $\mathscr{A}$, $\mathscr{B}$ and $\mathscr{C}$, which implicitly depend on $\mathbf{q}$, $\mathbf{v}$, $\dot{\mathbf{v}}$ and $\boldsymbol{\lambda}$, the equations of motion can be represented in three equivalent ways as

- the formulation with the constraints at position level:

$$\dot{\mathbf{q}} = \mathbf{v} \tag{11a}$$

$$\mathbf{M}(\mathbf{q}) \dot{\mathbf{v}} - \mathbf{g}_{\mathbf{q}}^T(\mathbf{q}) \boldsymbol{\lambda} = \mathbf{f}(\mathbf{q}, \mathbf{v}, t) \tag{11b}$$

$$\mathbf{g}^{\mathscr{A}}(\mathbf{q}) = \mathbf{0} \tag{11c}$$

$$\boldsymbol{\lambda}^{\overline{\mathscr{A}}} = \mathbf{0} \tag{11d}$$

- the formulation with the constraints at velocity level:

$$\dot{\mathbf{q}} = \mathbf{v} \tag{12a}$$

$$\mathbf{M}(\mathbf{q})\dot{\mathbf{v}} - \mathbf{g}_{\mathbf{q}}^{T}(\mathbf{q})\boldsymbol{\lambda} = \mathbf{f}(\mathbf{q}, \mathbf{v}, t) \tag{12b}$$

$$\mathbf{g}_{\mathbf{q}}^{\mathscr{B}}(\mathbf{q})\mathbf{v} = \mathbf{0} \tag{12c}$$

$$\boldsymbol{\lambda}^{\overline{\mathscr{B}}} = \mathbf{0} \tag{12d}$$

- the formulation with the constraints at acceleration level:

$$\dot{\mathbf{q}} = \mathbf{v} \tag{13a}$$

$$\mathbf{M}(\mathbf{q})\dot{\mathbf{v}} - \mathbf{g}_{\mathbf{q}}^{T}(\mathbf{q})\boldsymbol{\lambda} = \mathbf{f}(\mathbf{q}, \mathbf{v}, t) \tag{13b}$$

$$\mathbf{g}_{\mathbf{q}}^{\mathscr{C}}(\mathbf{q})\dot{\mathbf{v}} + \mathbf{h}^{\mathscr{C}}(\mathbf{q}, \mathbf{v}) = \mathbf{0} \tag{13c}$$

$$\boldsymbol{\lambda}^{\overline{\mathscr{C}}} = \mathbf{0} \tag{13d}$$

The expression of the Lagrange multipliers can now be obtained from the formulation with the constraints at acceleration level. Indeed, if the mass matrix is nonsingular, the acceleration can be evaluated from Eq. (13b) as

$$\dot{\mathbf{v}} = \mathbf{M}^{-1}(\mathbf{q})\left(\mathbf{f}(\mathbf{q}, \mathbf{v}, t) + \mathbf{g}_{\mathbf{q}}^{T}(\mathbf{q})\boldsymbol{\lambda}\right) \tag{14}$$

so that Eqs. (13c) and (13d) give the equation for the Lagrange multipliers as

$$\mathbf{g}_{\mathbf{q}}^{\mathscr{C}}(\mathbf{q})\mathbf{M}^{-1}(\mathbf{q})\left(\mathbf{f}(\mathbf{q}, \mathbf{v}, t) + \mathbf{g}_{\mathbf{q}}^{T}(\mathbf{q})\boldsymbol{\lambda}\right) + \mathbf{h}^{\mathscr{C}}(\mathbf{q}, \mathbf{v}) = \mathbf{0} \tag{15a}$$

$$\boldsymbol{\lambda}^{\overline{\mathscr{C}}} = \mathbf{0} \tag{15b}$$

If the position $\mathbf{q}(t)$ and velocity $\mathbf{v}(t)$ are known at a given time t and if all constraints in $\mathscr{C}$ are independent, the Lagrange multipliers $\boldsymbol{\lambda}(t)$ can be evaluated by solving this linear set of algebraic equations. Actually, this problem includes a linear complementarity condition as the active set $\mathscr{C}$ implicitly depends on the unknown value of $\boldsymbol{\lambda}(t)$.

This constraint differentiation process revealed the existence of hidden bilateral and unilateral constraints at position, velocity and acceleration levels, which are satisfied by the exact solution. Clearly, the initial conditions $\mathbf{q}_0$ and $\mathbf{v}_0$ should be consistent with the constraints at position and velocity levels. In the context of DAE (i.e., systems without unilateral constraint), these hidden constraints are at the core of so-called index reduction methods which have been proposed to improve the numerical stability of time integration schemes [4]. In the context of unilaterally constrained systems, these hidden constraints can also be exploited to formulate efficient numerical algorithms as will be discussed later.

2.2 Mechanical systems with impacts

2.2.1 Equations of motion

Now, the formulation is extended to deal with impact phenomena which means that impulsive reaction forces and jumps in the velocity field may arise, though the position field remains continuous in time. Assuming that the velocity is a function of bounded variation, the right and left limits are introduced

$$\dot{\mathbf{q}}^+(t) = \lim_{\tau \to t, \tau > t} \dot{\mathbf{q}}(\tau) \tag{16}$$

$$\dot{\mathbf{q}}^-(t) = \lim_{\tau \to t, \tau < t} \dot{\mathbf{q}}(\tau) \tag{17}$$

$$\mathbf{v}^+(t) = \lim_{\tau \to t, \tau > t} \mathbf{v}(\tau) \tag{18}$$

$$\mathbf{v}^-(t) = \lim_{\tau \to t, \tau < t} \mathbf{v}(\tau) \tag{19}$$

For the sake of notation simplicity, the convention $\mathbf{v}(t) = \mathbf{v}^+(t)$ and $\dot{\mathbf{q}}(t) = \dot{\mathbf{q}}^+(t)$ shall be used in the remaining part of this chapter.

When an impact occurs, the velocity is discontinuous and the acceleration is not well-defined in the usual sense. This motivates the representation of the dynamics in terms of the measure associated with the velocity $d\mathbf{v}$ [26]. This measure satisfies the property

$$\mathbf{v}(t_2) - \mathbf{v}(t_1) = \int_{(t_1, t_2]} d\mathbf{v} \tag{20}$$

and, if the singular continuous part of the measure is neglected, it admits the decomposition

$$d\mathbf{v} = \dot{\mathbf{v}} \, dt + \sum_i (\mathbf{v}(t_i) - \mathbf{v}^-(t_i)) \, \delta_{t_i} \tag{21}$$

where dt is the standard Lebesgue measure, the summation is performed over all impacts and δ_{t_i} is the Dirac delta supported at t_i. Similarly, a measure $d\mathbf{i}$ is introduced to represent the reaction forces with possible impulsive contributions. This measure is such that the integral

$$\boldsymbol{\Lambda}^*(t_1; t_2) = \int_{(t_1, t_2]} d\mathbf{i} \tag{22}$$

represents the total impulse of the reaction forces over the time interval $(t_1, t_2]$ and it admits the decomposition

$$d\mathbf{i} = \boldsymbol{\lambda} \, dt + \sum_i \mathbf{p}_i \, \delta_{t_i} \tag{23}$$

where $\boldsymbol{\lambda}$ is the vector of nonimpulsive Lagrange multipliers associated with the Lebesgue measurable constraint forces and $\mathbf{p}_i$ is the impulse producing the jump at the instant t_i.

Then, the equations of motion can be expressed in the following form

$$\dot{\mathbf{q}} = \mathbf{v} \tag{24a}$$

$$\mathbf{M}(\mathbf{q})\,\mathrm{d}\mathbf{v} - \mathbf{g}_{\mathbf{q}}^{T}(\mathbf{q})\,\mathrm{d}\mathbf{i} = \mathbf{f}(\mathbf{q},\mathbf{v},t)\,\mathrm{d}t \tag{24b}$$

$$\mathbf{g}^{\overline{\mathscr{U}}}(\mathbf{q}) = \mathbf{0} \tag{24c}$$

$$\mathbf{0} \leq \mathbf{g}^{\mathscr{U}}(\mathbf{q}(t)) \perp \mathrm{d}\mathbf{i}^{\mathscr{U}} \geq \mathbf{0} \tag{24d}$$

2.2.2 Impact equation

For almost every time t, when there is no impact, the equations of motion given in Eq. (11) with the definition of the active unilateral constraint $\mathscr{U}_A$ in Eq. (6) are still valid. At each impact time t_i, Eq. (24d) leads to

$$\mathbf{0} \leq \mathbf{g}^{\mathscr{U}}(\mathbf{q}(t_i)) \perp \mathbf{p}_{i}^{\mathscr{U}} \geq \mathbf{0} \tag{25}$$

so that the definition of the set of active unilateral constraints $\mathscr{U}_A$ at the impact time t_i is adapted as

$$\mathscr{U}_A(t_i) = \{j \in \mathscr{U} : p_i^j - r_p\, g^j(\mathbf{q}(t_i)) \geq 0\} \tag{26}$$

with the strictly positive scalar number $r_p > 0$. The equations of motion at the impact time become

$$\mathbf{M}(\mathbf{q}(t_i))\,(\mathbf{v}(t_i) - \mathbf{v}^-(t_i)) - \mathbf{g}_{\mathbf{q}}^{T}(\mathbf{q}(t_i))\,\mathbf{p}_i = \mathbf{0} \tag{27a}$$

$$\mathbf{g}^{\mathscr{A}}(\mathbf{q}(t_i)) = \mathbf{0} \tag{27b}$$

$$\mathbf{p}_i^{\overline{\mathscr{A}}} = \mathbf{0} \tag{27c}$$

An impact law is then needed to specify the post-impact velocity. The Newton impact law defines the normal velocity jump in case of an impact for the constraint $j \in \mathscr{U}_A(t_i)$ as

$$g_{\mathbf{q}}^j(\mathbf{q}(t_i))\,\mathbf{v}(t_i) = -e^j\, g_{\mathbf{q}}^j(\mathbf{q}(t_i))\,\mathbf{v}^-(t_i) \tag{28}$$

where $e^j \in [0,1]$ is the coefficient of restitution. The present formalism is developed for the analysis of contact conditions between rigid or flexible bodies. For rigid bodies, the coefficient of restitution defines the amount of energy dissipated during an impact. For flexible bodies, the physical meaning of a coefficient of restitution is not clear. The spatial discretization of a flexible body using the finite element method leads to a finite dimensional system with finite masses. An impact law with a coefficient of restitution is thus needed to describe contact conditions. In practice, for flexible bodies, a value $e^j = 0$ may be used so that the condition $g_{\mathbf{q}}^j \mathbf{v}(t_i) = 0$ is imposed when the constraint is active. Based on this impact law, the contact condition at the impact time is expressed at velocity level as

$$\mathbf{0} \leq \mathbf{g}_{\mathbf{q}}^{\mathscr{U}_A}(\mathbf{q}(t_i))\,\mathbf{v}(t_i) + \mathbf{E}^{\mathscr{U}_A}\,\mathbf{g}_{\mathbf{q}}^{\mathscr{U}_A}(\mathbf{q}(t_i))\,\mathbf{v}^-(t_i) \perp \mathbf{p}_i^{\mathscr{U}_A} \geq \mathbf{0} \tag{29}$$

where $\mathbf{E}^{\mathscr{U}}$ is a diagonal matrix formed with the coefficients of restitutions of all contact points. At the impact time t_i, the set of active unilateral constraints at velocity

level $\mathscr{U}_B$ is adapted as

$$\mathscr{U}_B(t_i) = \left\{ j \in \mathscr{U}_A(t_i) : p_i^j - r_p \left(g_{\mathbf{q}}^j(\mathbf{q}(t_i)) \, \mathbf{v}(t_i) + e^j \, g_{\mathbf{q}}^j(\mathbf{q}(t_i)) \, \mathbf{v}^-(t_i) \right) \geq 0 \right\} \quad (30)$$

The equation to evaluate the velocity jump and the impact at time t_i is obtained as

$$\mathbf{M}(\mathbf{q}(t_i)) \, (\mathbf{v}(t_i) - \mathbf{v}^-(t_i)) - \mathbf{g}_{\mathbf{q}}^T(\mathbf{q}(t_i)) \, \mathbf{p}_i = \mathbf{0} \tag{31a}$$

$$\mathbf{g}_{\mathbf{q}}^{\mathscr{B}}(\mathbf{q}(t_i)) \, \mathbf{v}(t_i) + \mathbf{E}^{\mathscr{B}} \, \mathbf{g}_{\mathbf{q}}^{\mathscr{B}}(\mathbf{q}(t_i)) \, \mathbf{v}^-(t_i) = \mathbf{0} \tag{31b}$$

$$\mathbf{p}_i^{\overline{\mathscr{B}}} = \mathbf{0} \tag{31c}$$

Equation (31b) accounts for the bilateral and active unilateral constraints. The size of the matrix of restitution coefficients $\mathbf{E}$ is thus adapted to include the bilateral constraints with artificial restitution coefficients fixed to zero.

2.2.3 Active set formulations

The definitions of $\mathscr{U}_A$ in Eqs. (6) and (26) can be merged in a single definition valid for every time as

$$\mathscr{U}_A = \{ j \in \mathscr{U} : di^j - g^j(\mathbf{q}) \, d\rho \geq 0 \} \tag{32}$$

where $d\rho > 0$ is a measure defined from the strictly positive and constant scalar numbers r and r_p as

$$d\rho = r \, dt + r_p \sum_i \delta_{t_i} \tag{33}$$

Then, the combination of Eq. (11) and Eq. (27) leads to a formulation in terms of measures

$$\dot{\mathbf{q}} = \mathbf{v} \tag{34a}$$

$$\mathbf{M}(\mathbf{q}(t)) \, d\mathbf{v} - \mathbf{g}_{\mathbf{q}}^T(\mathbf{q}) \, d\mathbf{i} = \mathbf{f}(\mathbf{q}, \mathbf{v}, t) \, dt \tag{34b}$$

$$\mathbf{g}^{\mathscr{A}}(\mathbf{q}(t)) = \mathbf{0} \tag{34c}$$

$$d\mathbf{i}^{\overline{\mathscr{A}}} = \mathbf{0} \tag{34d}$$

which is valid for every time and in which the constraints are expressed at position level. Notice that Eq. (34) should be combined with the impact law to obtain a complete set of equations.

Similarly, the definitions of $\mathscr{U}_B$ in Eq. (8) and (30) can be merged in a single definition for every time as

$$\mathscr{U}_B = \left\{ j \in \mathscr{U}_A : di^j - (g_{\mathbf{q}}^j(\mathbf{q}) \, \mathbf{v} + e^j \, g_{\mathbf{q}}^j(\mathbf{q}) \, \mathbf{v}^-) \, d\rho \geq 0 \right\} \tag{35}$$

Then, the formulation of the equations of motion in terms of measures is obtained from Eqs. (12) and (31) as

$$\dot{\mathbf{q}} = \mathbf{v} \tag{36a}$$

$$\mathbf{M}(\mathbf{q}(t))\, \mathrm{d}\mathbf{v} - \mathbf{g}_{\mathbf{q}}^T(\mathbf{q})\, \mathrm{d}\mathbf{i} = \mathbf{f}(\mathbf{q}, \mathbf{v}, t)\, \mathrm{d}t \tag{36b}$$

$$\mathbf{g}_{\mathbf{q}}^{\mathscr{B}}(\mathbf{q})\, \mathbf{v} + \mathbf{E}^{\mathscr{B}}\, \mathbf{g}_{\mathbf{q}}^{\mathscr{B}}(\mathbf{q})\, \mathbf{v}^- = \mathbf{0} \tag{36c}$$

$$\mathrm{d}\mathbf{i}^{\overline{\mathscr{B}}} = \mathbf{0} \tag{36d}$$

which is valid for every time and in which the constraints are expressed at velocity level.

As in the Moreau-Jean method, the formulation in Eq. (36) embeds the impact law in the expression of the constraints at velocity level. However, the activation criterion defined by Eqs. (32) and (35) involves the augmented Lagrange multipliers $\mathrm{d}i^j - g^j\,\mathrm{d}\rho$ and thereby differs from the activation strategy initially proposed by Moreau which only involves the gap distance g^j. In our notations, the set of active unilateral constraints in the original Moreau-Jean method would be defined as

$$\mathscr{U}_A^{\mathrm{Moreau}}(t) = \{ j \in \mathscr{U} : g^j(\mathbf{q}(t)) \le 0 \} \tag{37}$$

After time discretization, the set $\mathscr{U}_A^{\mathrm{Moreau}}$ at time step t_{n+1} is evaluated based on a prediction of the displacement $\mathbf{q}^*(t_{n+1})$ whose definition affects the numerical solution. In practice, it turns out that, in the Moreau-Jean method, $\mathbf{q}^*(t_{n+1})$ cannot be merely chosen as the actual displacement $\mathbf{q}(t_{n+1})$. In contrast, we will show that the proposed activation criterion based on augmented Lagrange multipliers according to Eqs. (6) and (26) leads to a simpler and more implicit discrete activation strategy.

Equation (36) can be discretized in time using the Moreau-Jean θ-method [25, 27]. This method is known for its robustness and its ability to deal consistently with unilateral constraints and impacts in mechanical systems. However, as the constraints are only imposed at velocity level, the numerical integration error will induce a drift of the constraints at position level which will accumulate as time goes by. Also, for standard applications, the numerical parameter θ is selected in the interval $(1/2, 1]$. This implies that the equations of motion are integrated with only first-order accuracy and that the overall solution is affected by a rather large level of numerical dissipation.

For nonsmooth systems, it is not possible to formulate the equations of motion in terms of measures with the constraints at acceleration level because the acceleration variable is only defined for almost every time but not at the impact instants.

3 Nonsmooth generalized-α method

3.1 Splitting method

Following [12, 14], the motion is splitted at one time step into a smooth trajectory with continuous positions and velocities and nonsmooth contributions representing impulsive forces, velocity jumps and position corrections. The smooth trajectory is

constructed by integration of an acceleration variable $\dot{\tilde{\mathbf{v}}}$ that shall be defined below. The advantage of this approach comes from the possibility to use a second-order scheme to integrate $\dot{\tilde{\mathbf{v}}}$ instead of a first-order θ-method.

Let us introduce the set of constraints $\mathscr{S}(t)$ that shall be included in the definition of the smooth motion. It can be selected in several different manners which shall be studied later in Section 3.2. At a given time t and for given values of $\mathbf{q}(t)$ and $\mathbf{v}(t)$, the smooth acceleration $\dot{\tilde{\mathbf{v}}}(t)$ and the smooth Lagrange multiplier $\tilde{\boldsymbol{\lambda}}(t)$ are defined as the solution of the well-posed algebraic system

$$\mathbf{M}(\mathbf{q})\,\dot{\tilde{\mathbf{v}}} - \mathbf{g}_{\mathbf{q}}^{T}(\mathbf{q})\,\tilde{\boldsymbol{\lambda}} = \mathbf{f}(\mathbf{q},\mathbf{v},t) \tag{38a}$$

$$\mathbf{g}_{\mathbf{q}}^{\mathscr{S}}(\mathbf{q})\,\dot{\tilde{\mathbf{v}}} + \mathbf{h}^{\mathscr{S}}(\mathbf{q},\mathbf{v}) = \mathbf{0} \tag{38b}$$

$$\tilde{\boldsymbol{\lambda}}^{\overline{\mathscr{S}}} = \mathbf{0} \tag{38c}$$

An important point is that the resulting acceleration $\dot{\tilde{\mathbf{v}}}(t)$ is defined for every time, including the impact instants. The values of $\dot{\tilde{\mathbf{v}}}$ and $\tilde{\boldsymbol{\lambda}}$ at time t only depend on the values of $\mathbf{q}$, $\mathbf{v}$ and $\mathscr{S}$ at time t. In general, $\mathscr{S}(t)$ implicitly depends on $\dot{\tilde{\mathbf{v}}}(t)$ and $\tilde{\boldsymbol{\lambda}}(t)$. As $\mathbf{q}(t)$ is a continuous function and $\mathbf{v}(t)$ is a function of bounded variations, the acceleration $\dot{\tilde{\mathbf{v}}}(t)$ and the multiplier $\tilde{\boldsymbol{\lambda}}(t)$ are also functions of bounded variations and, by construction, they are free from any impulsive contribution. Also, we use the conventions $\dot{\tilde{\mathbf{v}}}(t) = \dot{\tilde{\mathbf{v}}}^{+}(t)$ and $\tilde{\boldsymbol{\lambda}}(t) = \tilde{\boldsymbol{\lambda}}^{+}(t)$. Notice that a discontinuity of $\dot{\tilde{\mathbf{v}}}(t)$ can be either caused by a jump in the velocity $\mathbf{v}(t)$ or by a constraint activation or deactivation in the set $\mathscr{S}(t)$. The velocity field $\tilde{\mathbf{v}}(t)$ and the position field $\tilde{\mathbf{q}}(t)$ of the smooth trajectory, which are obtained by time integration of $\dot{\tilde{\mathbf{v}}}(t)$ over the time step, are continuous functions of time.

The nonsmooth contributions to the total motion are then represented by the differential measure $d\mathbf{w}$, which is defined such that

$$d\mathbf{v} = \dot{\tilde{\mathbf{v}}}\,dt + d\mathbf{w} \tag{39}$$

We obtain using Eqs . (36b), (38a) and (39)

$$\mathbf{M}(\mathbf{q})\,d\mathbf{w} - \mathbf{g}_{\mathbf{q}}^{T}(\mathbf{q})\,(d\mathbf{i} - \tilde{\boldsymbol{\lambda}}\,dt) = \mathbf{0} \tag{40}$$

We insist on the fact that the smooth trajectory is a mere artificial construction which is only intended to the formulation of an appropriate time integration procedure. The physical response is represented by the total motion $\mathbf{q}(t)$ and $\mathbf{v}(t)$ and the total impulse $d\mathbf{i}$.

The formulation of the constraints at acceleration level in Eq. (38b) departs from the definition of the smooth motion based on the velocity constraints that was proposed in [12] but leads to several advantages that will be investigated throughout the paper. Firstly, it is not necessary to evaluate explicitly the smooth trajectory at position or velocity levels, which simplifies the initialization of these variables. Secondly, the sensitivity of this formulation to disturbances induced by the coupling with nonsmooth phenomena, such as velocity jumps or constraint activation and de-

activation, is reduced. Thirdly, this formulation can tolerate the dynamic activation and deactivation of unilateral constraints in the set $\mathscr{S}(t)$.

In summary, the dynamics is now represented by the following set of equations

$$\dot{\mathbf{q}} = \mathbf{v} \tag{41a}$$

$$d\mathbf{v} = \dot{\mathbf{v}}\,dt + d\mathbf{w} \tag{41b}$$

$$\mathbf{M}(\mathbf{q})\,\dot{\mathbf{v}} - \mathbf{g}_{\mathbf{q}}^{T}(\mathbf{q})\,\tilde{\boldsymbol{\lambda}} = \mathbf{f}(\mathbf{q},\mathbf{v},t) \tag{41c}$$

$$\mathbf{g}_{\mathbf{q}}^{\mathscr{S}}(\mathbf{q})\,\dot{\mathbf{v}} + \mathbf{h}^{\mathscr{S}}(\mathbf{q},\mathbf{v}) = \mathbf{0} \tag{41d}$$

$$\tilde{\boldsymbol{\lambda}}^{\overline{\mathscr{S}}} = \mathbf{0} \tag{41e}$$

$$\mathbf{M}(\mathbf{q})\,d\mathbf{w} - \mathbf{g}_{\mathbf{q}}^{T}(\mathbf{q})\,(d\mathbf{i} - \tilde{\boldsymbol{\lambda}}\,dt) = \mathbf{0} \tag{41f}$$

$$\mathbf{g}_{\mathbf{q}}^{\mathscr{B}}(\mathbf{q})\,\mathbf{v} + \mathbf{E}^{\mathscr{B}}\,\mathbf{g}_{\mathbf{q}}^{\mathscr{B}}(\mathbf{q}^{-})\,\mathbf{v}^{-} = \mathbf{0} \tag{41g}$$

$$d\mathbf{i}^{\overline{\mathscr{B}}} = \mathbf{0} \tag{41h}$$

3.2 Activation strategy for the constraints on the smooth motion

This section addresses the possible contribution $\tilde{\boldsymbol{\lambda}}$ of the constraint reaction forces in the definition of the smooth motion. The choice to include such contributions or not bears some arbitrariness. Indeed, the value of $\tilde{\boldsymbol{\lambda}}$ has no physical meaning, only the total impulse represented by $d\mathbf{i}$ can receive a physical interpretation. Even though some contributions of the reaction forces are disregarded in the definition of $\tilde{\boldsymbol{\lambda}}$, they will be consistently incorporated in the the total impulse $d\mathbf{i}$ which satisfies the discrete complementarity condition.

However, it is appealing to define the smooth motion so that it evolves as close as possible to the physical motion for at least two reasons. Firstly, the smooth motion is integrated using a higher-order scheme, so we can expect a higher accuracy if the smooth motion is closer to the total (physical) one. Secondly, when the nonsmooth corrections are reduced, the convergence of the iterative procedure at each time step, which is at the core of the implicit integration procedure, is accelerated.

In the proposed method, the acceleration $\dot{\mathbf{v}}$ and the multipliers $\tilde{\boldsymbol{\lambda}}$ are well-defined at any time (though they can be discontinuous) by Eq. (38) so that, by construction, no impulsive term can appear. This observation remains valid when some constraints on the smooth motion are activated and deactivated. This means that we are relatively free to dynamically activate and deactivate some unilateral constraints in $\mathscr{S}$ as we feel appropriate without inducing inconsistent impulsive excitations on the smooth motion.

Three different activation strategies for the smooth constraints are now considered.

- Strategy 1: $\mathscr{S} = \emptyset$, i.e., no bilateral constraint and no unilateral constraint is taken into account, as proposed in [14]. This means that the smooth motion is considered as a constraint-free motion.

- Strategy 2: $\mathscr{S} = \overline{\mathscr{U}}$, i.e., only the bilateral constraints are taken into account but all unilateral constraints are excluded, as proposed in [12]. This means that the smooth motion satisfies the bilateral constraints but does not account for the contact forces.
- Strategy 3: $\mathscr{S} = \overline{\mathscr{U}} \cup \tilde{\mathscr{U}}_C$, with $\tilde{\mathscr{U}}_C$ the time-dependent set of active unilateral constraints at acceleration level defined according to

$$\tilde{\mathscr{U}}_C = \{ j \in \mathscr{U}_B : \lambda^j - r(g_{\mathbf{q}}^j(\mathbf{q})\,\dot{\tilde{\mathbf{v}}} + h^j(\mathbf{q},\mathbf{v})) \geq 0 \} \tag{42}$$

This strategy is a new approach considered in this chapter. Notice that the definition of $\tilde{\mathscr{U}}_C$ relies on the acceleration $\dot{\tilde{\mathbf{v}}}$ which is well-posed for every time (including the impact times) and thus slightly differs from the definition of $\mathscr{U}_C$ which is not defined at the impact time. With this strategy, for almost every time (when there is no impact), Eqs. (13) and (38) are strictly equivalent so that $\dot{\tilde{\mathbf{v}}} = \dot{\mathbf{v}}$ and $\tilde{\boldsymbol{\lambda}} = \boldsymbol{\lambda}$. This means that, for almost every time, $\dot{\tilde{\mathbf{v}}}$ and $\tilde{\boldsymbol{\lambda}}$ represent the standard accelerations and reaction forces but that they exclude impulsive contributions at the impact instants.

Compared to strategy 1, we clearly expect that strategy 2 brings the smooth motion closer to the physical motion as it satisfies the bilateral constraints. For this reason, strategy 2 should be preferred to strategy 1.

When all active unilateral constraints remain closed, the physical motion becomes smooth and satisfies the active constraints at acceleration level. In this case, for the exact solution, the smooth motion defined in strategy 3 is equal to the total motion, i.e., $\dot{\tilde{\mathbf{v}}} = \dot{\mathbf{v}}$ and $\tilde{\boldsymbol{\lambda}} = \boldsymbol{\lambda}$. This means that the total motion is integrated with second-order accuracy. In the numerical scheme, numerical errors may lead to small differences between the smooth motion and the total motion but we expect that these differences are much smaller compared to the position corrections and velocity jumps in strategy 2. Compared to strategy 2, strategy 3 should thus be preferred when the constraints remain closed.

When some unilateral constraints are active but some impulsive phenomena are present in the system, the acceleration is not well-defined and the physical interpretation of the constraint at acceleration level becomes irrelevant. In this case, it is not clear whether strategy 2 or strategy 3 should be preferred. This question will be investigated through numerical tests in Section 6.

3.3 Gear-Gupta-Leimkuhler formulation

In Eq. (41g), the constraints on the total (physical) motion are imposed at velocity level. Due to numerical integration errors, a drift of the constraints is expected at position level. In order to remedy this situation, an adaptation of the Gear-Gupta-Leimkuhler formulation [18] to nonsmooth systems was considered by several authors [1, 12, 36]. The algorithm discussed here is built upon the formulation proposed in [12]. An additional Lagrange multiplier $\boldsymbol{\mu}$ is thus introduced in Eq. (41a)

leading to

$$\mathrm{d}\mathbf{v} = \dot{\mathbf{v}}\,\mathrm{d}t + \mathrm{d}\mathbf{w} \tag{43a}$$

$$\mathbf{M}(\mathbf{q})\dot{\mathbf{v}} - \mathbf{g}_{\mathbf{q}}^{T}(\mathbf{q})\tilde{\boldsymbol{\lambda}} = \mathbf{f}(\mathbf{q},\mathbf{v},t) \tag{43b}$$

$$\mathbf{g}_{\mathbf{q}}^{\mathscr{S}}(\mathbf{q})\dot{\mathbf{v}} + \mathbf{h}^{\mathscr{S}}(\mathbf{q},\mathbf{v}) = \mathbf{0} \tag{43c}$$

$$\tilde{\boldsymbol{\lambda}}^{\overline{\mathscr{S}}} = \mathbf{0} \tag{43d}$$

$$\mathbf{M}(\mathbf{q})(\dot{\mathbf{q}} - \mathbf{v}) - \mathbf{g}_{\mathbf{q}}^{T}(\mathbf{q})\boldsymbol{\mu} = \mathbf{0} \tag{43e}$$

$$\mathbf{g}^{\mathscr{A}}(\mathbf{q}) = \mathbf{0} \tag{43f}$$

$$\boldsymbol{\mu}^{\overline{\mathscr{A}}} = \mathbf{0} \tag{43g}$$

$$\mathbf{M}(\mathbf{q})\,\mathrm{d}\mathbf{w} - \mathbf{g}_{\mathbf{q}}^{T}(\mathbf{q})\,(\mathrm{d}\mathbf{i} - \tilde{\boldsymbol{\lambda}}\,\mathrm{d}t) = \mathbf{0} \tag{43h}$$

$$\mathbf{g}_{\mathbf{q}}^{\mathscr{B}}(\mathbf{q})\,\mathbf{v} + \mathbf{E}^{\mathscr{B}}\,\mathbf{g}_{\mathbf{q}}^{\mathscr{B}}(\mathbf{q}^{-})\,\mathbf{v}^{-} = \mathbf{0} \tag{43i}$$

$$\mathrm{d}\mathbf{i}^{\overline{\mathscr{B}}} = \mathbf{0} \tag{43j}$$

One can easily check that the solution of Eq. (41) also satisfies Eq. (43) with $\boldsymbol{\mu} = \mathbf{0}$. So the introduction of the new Lagrange multiplier preserves the original solution of the problem.

3.4 Discrete smooth and nonsmooth variables

In order to prepare the time discretization procedure, several global variables which represent the total jumps and total impulses over the time step $(t_n, t_{n+1}]$ are introduced. Over the current time step, the smooth motion is first constructed by integration of the smooth acceleration $\dot{\mathbf{v}}(t)$ from the physical initial conditions $\mathbf{q}(t_n)$ and $\mathbf{v}(t_n)$ to the end of the time step

$$\tilde{\mathbf{v}}(t) = \mathbf{v}(t_n) + \int_{t_n}^{t} \dot{\mathbf{v}}(\tau)\,\mathrm{d}\tau \tag{44}$$

$$\tilde{\mathbf{q}}(t_{n+1}) = \mathbf{q}(t_n) + h\,\mathbf{v}(t_n) + \int_{t_n}^{t_{n+1}} \int_{t_n}^{t} \dot{\mathbf{v}}(\tau)\,\mathrm{d}\tau\,\mathrm{d}t \tag{45}$$

where $h = t_{n+1} - t_n$ is the the time-step size. Even if the total velocity $\mathbf{v}(t)$ undergoes a discontinuity, $\tilde{\mathbf{v}}(t)$ is by construction a continuous function of time in $(t_n, t_{n+1}]$.

The velocity jump is defined as

$$\mathbf{W}(t_n; t_{n+1}) = \int_{(t_n, t_{n+1}]} \mathrm{d}\mathbf{w} \tag{46}$$

Using Eqs. (39) and (44), we get

$$\mathbf{W}(t_n; t_{n+1}) = \mathbf{v}(t_{n+1}) - \tilde{\mathbf{v}}(t_{n+1}) \tag{47}$$

Similarly, the position correction is defined as

$$\mathbf{U}(t_n;t_{n+1}) = \int_{t_n}^{t_{n+1}} \left(\dot{\mathbf{q}}(t) - \tilde{\mathbf{v}}(t) \right) \mathrm{d}t \tag{48}$$

so that using Eqs. (39), (44) and (45)

$$\mathbf{U}(t_n;t_{n+1}) = \mathbf{q}(t_{n+1}) - \tilde{\mathbf{q}}(t_{n+1}) \tag{49}$$

Then, the relative impulse variable

$$\boldsymbol{\Lambda}(t_n;t_{n+1}) = \int_{(t_n,t_{n+1}]} \left(\mathrm{d}\mathbf{i} - \tilde{\boldsymbol{\lambda}}(t)\,\mathrm{d}t \right) \tag{50}$$

and the relative double integral variable

$$\boldsymbol{v}(t_n;t_{n+1}) = \int_{t_n}^{t_{n+1}} \left(\boldsymbol{\mu}(t) + \int_{(t_n,t]} (\mathrm{d}\mathbf{i} - \tilde{\boldsymbol{\lambda}}(t)\,\mathrm{d}\tau) \right) \mathrm{d}t \tag{51}$$

are introduced so that, according to Theorem 1 in [12],

$$\mathbf{M}(\mathbf{q}(t_{n+1}))\,\mathbf{W}(t_n;t_{n+1}) - \mathbf{g}_{\mathbf{q}}^{T}(\mathbf{q}(t_{n+1}))\,\boldsymbol{\Lambda}(t_n;t_{n+1}) = \mathscr{O}(h) \tag{52a}$$

$$\mathbf{M}(\mathbf{q}(t_{n+1}))\,\mathbf{U}(t_n;t_{n+1}) - \mathbf{g}_{\mathbf{q}}^{T}(\mathbf{q}(t_{n+1}))\,\boldsymbol{v}(t_n;t_{n+1}) = \mathscr{O}(h^2) \tag{52b}$$

It is important to observe that $\boldsymbol{\Lambda}(t_n;t_{n+1})$ does not represent the total impulse of the reaction forces but only a part of it as the contribution of the non-impulsive reaction forces $\tilde{\boldsymbol{\lambda}}$ is excluded in the definition (50). The total (physical) impulse, denoted as $\boldsymbol{\Lambda}^*(t_n;t_{n+1})$, is evaluated by time integration of the measure of the reaction forces $\mathrm{d}\mathbf{i}$

$$\boldsymbol{\Lambda}^*(t_n;t_{n+1}) = \int_{(t_n,t_{n+1}]} \mathrm{d}\mathbf{i} = \boldsymbol{\Lambda}(t_{n+1}) + \int_{t_n}^{t_{n+1}} \tilde{\boldsymbol{\lambda}}(t)\,\mathrm{d}t \tag{53}$$

Similarly, the total double integral $\boldsymbol{v}^*(t_n;t_{n+1})$ is defined as

$$\boldsymbol{v}^*(t_n;t_{n+1}) = \int_{t_n}^{t_{n+1}} \left(\boldsymbol{\mu}(t) + \int_{(t_n,t]} \mathrm{d}\mathbf{i} \right) \mathrm{d}t = \boldsymbol{v}(t_{n+1}) + \int_{t_n}^{t_{n+1}} \int_{t_n}^{t} \tilde{\boldsymbol{\lambda}}(t)\,\mathrm{d}\tau\,\mathrm{d}t \tag{54}$$

The contribution of $\boldsymbol{\mu}$ is introduced in Eq. (54) so that $\boldsymbol{v}^*(t_n;t_{n+1})$ is conveniently expressed in terms of the variables $\boldsymbol{v}(t_n;t_{n+1})$ and $\tilde{\boldsymbol{\lambda}}$.

3.5 Active sets in the discrete time system

Following a similar argumentation as developed in [12], the set of active unilateral constraints at position level over the time step $(t_n,t_{n+1}]$ is defined as

$$\mathscr{U}_A(t_n;t_{n+1}) = \left\{ j \in \mathscr{U} : v^{*j}(t_n;t_{n+1}) - r\,g^j(\mathbf{q}(t_{n+1})) \geq 0 \right\} \tag{55}$$

This activation rule based on the augmented Lagrange multiplier fixes the problem of the spurious oscillations reported in [1] in a simple way.

The active unilateral constraints at velocity level over the time step $(t_n, t_{n+1}]$ are defined as

$$\mathscr{U}_B(t_n; t_{n+1}) = \left\{ j \in \mathscr{U}_A(t_n; t_{n+1}) : \Lambda^{*j}(t_n; t_{n+1}) - r(g_{\mathbf{q}}^j \mathbf{v}(t_{n+1}) + e^j g_{\mathbf{q}}^j \mathbf{v}(t_n)) \geq 0 \right\} \tag{56}$$

Finally, if the third strategy is used for the activation of the constraints on the smooth motion (see Sect. 3.2), the active unilateral constraints at acceleration level over the time step $(t_n, t_{n+1}]$ are defined as

$$\mathscr{U}_C(t_n; t_{n+1}) = \{ j \in \mathscr{U}_B(t_n; t_{n+1}) : \\ \tilde{\lambda}^j(t_{n+1}) - r(g_{\mathbf{q}}^j \dot{\tilde{\mathbf{v}}}(t_{n+1}) + h^j(\mathbf{q}(t_{n+1}), \mathbf{v}(t_{n+1}))) \geq 0 \} \tag{57}$$

In [12], the unilateral constraints were never activated in the smooth equation so that $\tilde{\boldsymbol{\lambda}}^{\mathscr{U}} = \mathbf{0}$, $\mathbf{v}^{*\mathscr{U}} = \mathbf{v}^{\mathscr{U}}$ and $\boldsymbol{\Lambda}^{*\mathscr{U}} = \boldsymbol{\Lambda}^{\mathscr{U}}$. But if $\tilde{\boldsymbol{\lambda}}^{\mathscr{U}}$ differs from $\mathbf{0}$, it contributes directly to the physical contact forces. This is the reason why the activation criteria in Eqs. (55) and (56) need to be established based on the total impulse and total double integral represented by $\mathbf{v}^*$ and $\boldsymbol{\Lambda}^*$ (and not $\mathbf{v}$ and $\boldsymbol{\Lambda}$).

The definition of $\mathscr{U}_B$ also differs from [12] in the following way. Here, the definition of $\mathscr{U}_B$ involves the augmented Lagrange multipliers at position level (as it is a subset of $\mathscr{U}_A$) and a criterion on the augmented Lagrange multiplier at velocity level. In [12], the criterion on the augmented Lagrange multiplier at position level is replaced by a criterion on the penetration of the smooth motion $g^j(\tilde{\mathbf{q}}(t_{n+1})) \leq 0$. This modification allows us to completely eliminate the variable $\tilde{\mathbf{q}}$ from the algorithm and to simplify the formulation.

As discussed in [12], in this scheme, the variables $\mathbf{v}$ and $\mathbf{v}^*$ do not have a clear physical meaning but are only useful for the exact enforcement of all active constraints at position level at the end of the time step. So the physical contact impulse is solely represented by the variable $\boldsymbol{\Lambda}^*$.

3.6 Generalized-α time integration

The integrals in Eqs. (44) and (45) can be approximated according to the generalized-α method as

$$\int_{(t_n, t_{n+1}]} \dot{\mathbf{v}} \, dt = h(1 - \gamma)\mathbf{a}_n + h\gamma \mathbf{a}_{n+1} \tag{58}$$

$$\int_{t_n}^{t_{n+1}} \int_{t_n}^{t} \dot{\mathbf{v}}(\tau) \, d\tau \, dt = h^2(1 - \beta)\mathbf{a}_n + h^2 \beta \mathbf{a}_{n+1} \tag{59}$$

$$(1 - \alpha_m)\mathbf{a}_{n+1} + \alpha_m \mathbf{a}_n = (1 - \alpha_f)\dot{\mathbf{v}}_{n+1} + \alpha_f \dot{\mathbf{v}}_n \tag{60}$$

where $\mathbf{a}_{n+1}$ can be interpreted as a shifted approximation of the acceleration at time $t_{n+1} + (\alpha_m - \alpha_f)h$. In the initialization procedure, the value of $\mathbf{a}_0$ at time $t = 0$ can be approximated (i) by $\mathbf{a}_0 = \dot{\mathbf{v}}((\alpha_m - \alpha_f)h)$ by solving Eq. (38) at $t = (\alpha_m - \alpha_f)h$ or (ii) by the order h approximation $\mathbf{a}_0 = \dot{\mathbf{v}}(0)$. This second and simpler option is retained in this work. The numerical parameters β, γ, α_m, α_f can be selected according to the methods of Newmark [28], Hilber-Hughes-Taylor [21] or Chung and Hulbert [15]. This last option is considered here. The Chung-Hulbert method is a second-order scheme with an adjustable level of numerical dissipation in the high-frequency range. More precisely, based on the user-prescribed value of the spectral radius at infinite frequencies $\rho_\infty \in [0,1]$, which is an image of the level of numerical dissipation in the high-frequency range ($\rho_\infty = 1$ means no dissipation, $\rho_\infty = 0$ means maximal dissipation such that any high-frequency disturbance is eliminated in one time step), the coefficients of the Chung-Hulbert method are determined as

$$\alpha_m = \frac{2\rho_\infty - 1}{\rho_\infty + 1}, \ \alpha_f = \frac{\rho_\infty}{\rho_\infty + 1}, \ \gamma = 0.5 + \alpha_f - \alpha_m, \ \beta = 0.25(\gamma + 0.5)^2 \quad (61)$$

Finally, the integrals of the multipliers $\tilde{\boldsymbol{\lambda}}(t)$ that appear in the definition of the active sets $\mathscr{A}$ and $\mathscr{B}$ are evaluated using a similar strategy as

$$\int_{t_n}^{t_{n+1}} \tilde{\boldsymbol{\lambda}}(t)\,\mathrm{d}t = h(1-\gamma)\boldsymbol{\eta}_n + h\gamma\boldsymbol{\eta}_{n+1} \quad (62)$$

$$\int_{t_n}^{t_{n+1}} \int_{t_n}^{t} \tilde{\boldsymbol{\lambda}}(\tau)\,\mathrm{d}\tau\,\mathrm{d}t = h^2(1-\beta)\boldsymbol{\eta}_n + h^2\beta\boldsymbol{\eta}_{n+1} \quad (63)$$

$$(1-\alpha_m)\boldsymbol{\eta}_{n+1} + \alpha_m\boldsymbol{\eta}_n = (1-\alpha_f)\tilde{\boldsymbol{\lambda}}_{n+1} + \alpha_f\tilde{\boldsymbol{\lambda}}_n \quad (64)$$

where $\boldsymbol{\eta}_{n+1}$ is a shifted approximation of the multiplier $\tilde{\boldsymbol{\lambda}}$ at time $t_{n+1} + (\alpha_f - \alpha_m)h$, which is initialized as $\boldsymbol{\eta}_0 = \tilde{\boldsymbol{\lambda}}_0$.

3.7 Summary of the time stepping scheme

Based on the definitions and results presented in the previous sections, the discrete system of equations is finally obtained as

$$\mathbf{M}(\mathbf{q}_{n+1})\,\dot{\tilde{\mathbf{v}}}_{n+1} - \mathbf{g}_{\mathbf{q}}^T(\mathbf{q}_{n+1})\,\tilde{\boldsymbol{\lambda}}_{n+1} = \mathbf{f}(\mathbf{q}_{n+1},\mathbf{v}_{n+1},t_{n+1}) \tag{65a}$$

$$\mathbf{g}_{\mathbf{q}}^{\mathscr{S}}(\mathbf{q}_{n+1})\,\dot{\tilde{\mathbf{v}}}_{n+1} + \mathbf{h}^{\mathscr{S}}(\mathbf{q}_{n+1},\mathbf{v}_{n+1}) = \mathbf{0} \tag{65b}$$

$$\tilde{\boldsymbol{\lambda}}_{n+1}^{\overline{\mathscr{S}}} = \mathbf{0} \tag{65c}$$

$$\mathbf{M}(\mathbf{q}_{n+1})\mathbf{U}_{n+1} - \mathbf{g}_{\mathbf{q}}^T(\mathbf{q}_{n+1})\boldsymbol{\nu}_{n+1} = \mathbf{0} \tag{65d}$$

$$\mathbf{g}^{\mathscr{A}}(\mathbf{q}_{n+1}) = \mathbf{0} \tag{65e}$$

$$\boldsymbol{\nu}_{n+1}^{\overline{\mathscr{A}}} = \mathbf{0} \tag{65f}$$

$$\mathbf{M}(\mathbf{q}_{n+1})\mathbf{W}_{n+1} - \mathbf{g}_{\mathbf{q}}^T(\mathbf{q}_{n+1})\boldsymbol{\Lambda}_{n+1} = \mathbf{0} \tag{65g}$$

$$\mathbf{g}_{\mathbf{q}}^{\mathscr{B}}(\mathbf{q}_{n+1})\,\mathbf{v}_{n+1} + \mathbf{E}^{\mathscr{B}}\,\mathbf{g}_{\mathbf{q}}^{\mathscr{B}}(\mathbf{q}_n)\,\mathbf{v}_n = \mathbf{0} \tag{65h}$$

$$\boldsymbol{\Lambda}_{n+1}^{\overline{\mathscr{B}}} = \mathbf{0} \tag{65i}$$

combined with the time integration formulae

$$\mathbf{q}_{n+1} - \mathbf{q}_n = h\mathbf{v}_n + h^2(1-\beta)\mathbf{a}_n + h^2\beta\mathbf{a}_{n+1} + \mathbf{U}_{n+1} \tag{65j}$$

$$\mathbf{v}_{n+1} - \mathbf{v}_n = h(1-\gamma)\mathbf{a}_n + h\gamma\mathbf{a}_{n+1} + \mathbf{W}_{n+1} \tag{65k}$$

$$(1-\alpha_m)\mathbf{a}_{n+1} + \alpha_m\mathbf{a}_n = (1-\alpha_f)\dot{\tilde{\mathbf{v}}}_{n+1} + \alpha_f\dot{\tilde{\mathbf{v}}}_n \tag{65l}$$

The active sets $\mathscr{A}$, $\mathscr{B}$ and $\mathscr{S}$ are evaluated as described in Sect. 3.5 based on the discrete variables at time step $n+1$, in particular, based on the variables $\boldsymbol{\Lambda}_{n+1}^*$ and $\boldsymbol{\nu}_{n+1}^*$ defined as

$$\boldsymbol{\Lambda}_{n+1}^* = \boldsymbol{\Lambda}(t_{n+1}) + h(1-\gamma)\boldsymbol{\eta}_n + h\gamma\boldsymbol{\eta}_{n+1} \tag{65m}$$

$$\boldsymbol{\nu}_{n+1}^* = \boldsymbol{\nu}(t_{n+1}) + h^2(1-\beta)\boldsymbol{\eta}_n + h^2\beta\boldsymbol{\eta}_{n+1} \tag{65n}$$

$$(1-\alpha_m)\boldsymbol{\eta}_{n+1} + \alpha_m\boldsymbol{\eta}_n = (1-\alpha_f)\tilde{\boldsymbol{\lambda}}_{n+1} + \alpha_f\tilde{\boldsymbol{\lambda}}_n \tag{65o}$$

The sets $\mathscr{A}$, $\mathscr{B}$ and $\mathscr{S}$ thus implicitly depend on the solution at step t_{n+1}. Let us remark that the variables $\boldsymbol{\Lambda}_{n+1}^*$ and $\boldsymbol{\nu}_{n+1}^*$ do not explicitly appear in the equations of motion but are necessary for the definition of the active sets $\mathscr{A}$ and $\mathscr{B}$.

Initial conditions should be specified for the variables $\mathbf{q}_0$, $\mathbf{v}_0$, which should be compatible with the constraints at position and velocity levels. Based on these initial conditions, the initial values of $\dot{\tilde{\mathbf{v}}}_0$ and $\tilde{\boldsymbol{\lambda}}_0$ are obtained by solving the algebraic system (65a,65b,65c). Finally, one can initialize $\mathbf{a}_0 = \dot{\tilde{\mathbf{v}}}_0$ and $\boldsymbol{\eta}_0 = \tilde{\boldsymbol{\lambda}}_0$.

One also observes that the smooth positions $\tilde{\mathbf{q}}_{n+1}$ and velocities $\tilde{\mathbf{v}}_{n+1}$ do not appear in this scheme, which is a difference compared to the algorithm presented in [12].

3.8 Solution of the discretized problem

At each time step, the system of nonlinear equations represented by Eq. (65) should be solved for the different variables at time t_{n+1}. As the activation status of the con-

straints depends on the unknowns of the problem, the problem implicitly includes complementarity conditions.

For the sake of numerical efficiency, Eq. (65) can be condensed by elimination of the linear equations which represent the time integration formulae (65j-65o). This elimination relies on a distinction between the independent variables selected as $\dot{\tilde{\mathbf{v}}}_{n+1}$, $\tilde{\boldsymbol{\lambda}}_{n+1}$, $\mathbf{U}_{n+1}$, $\boldsymbol{\nu}_{n+1}$, $\mathbf{W}_{n+1}$, $\boldsymbol{\Lambda}_{n+1}$, and the remaining dependent variables $\mathbf{q}_{n+1}$, $\mathbf{v}_{n+1}$, $\mathbf{a}_{n+1}$, $\boldsymbol{\eta}_{n+1}$, $\boldsymbol{\nu}_{n+1}^*$ and $\boldsymbol{\Lambda}_{n+1}^*$. For a system with n_q coordinates in $\mathbf{q}$ and n_g constraints in $\mathbf{g}$, the problem is represented by a system of $3(n_q + n_g)$ nonlinear equations with complementarity conditions for the $3(n_q + n_g)$ independent variables.

Algorithm 1 Nonsmooth generalized-α time integration scheme

Inputs: initial values $\mathbf{q}_0$ and $\mathbf{v}_0$
Compute the consistent value of $\dot{\tilde{\mathbf{v}}}_0$ and $\tilde{\boldsymbol{\lambda}}_0$ and initialize $\mathbf{a}_0 := \dot{\tilde{\mathbf{v}}}_0$ and $\boldsymbol{\eta}_0 = \tilde{\boldsymbol{\lambda}}_0$
for $n = 0$ to $n_{\text{final}} - 1$ **do**
    Predict the variables $\mathbf{q}_{n+1}$, $\mathbf{v}_{n+1}$, $\dot{\tilde{\mathbf{v}}}_{n+1}$, $\boldsymbol{\nu}_{n+1}$, $\boldsymbol{\Lambda}_{n+1}$, $\tilde{\boldsymbol{\lambda}}_{n+1}$, $\mathbf{a}_{n+1}$, $\boldsymbol{\nu}_{n+1}^*$, $\boldsymbol{\eta}_{n+1}$ $\boldsymbol{\Lambda}_{n+1}^*$
    for $i = 1$ to i_{max} **do**
        Evaluate the sets $\mathscr{A}$, $\mathscr{B}$ and $\mathscr{S}$ at time t_{n+1}
        Evaluate the residuals of the equations of motion given by Eqs. (65a-65i)
        if all residuals are below the tolerance **then**
            break
        end if
        Evaluate the iteration matrix of Eqs. (65a,65b,65c) with respect to $\dot{\tilde{\mathbf{v}}}_{n+1}$ and $\tilde{\boldsymbol{\lambda}}_{n+1}$
        Solve the resulting linearized problem and evaluate the corrections of $\dot{\tilde{\mathbf{v}}}_{n+1}$ and $\tilde{\boldsymbol{\lambda}}_{n+1}$
        Update the dependent variables $\mathbf{q}_{n+1}$, $\mathbf{v}_{n+1}$, $\mathbf{a}_{n+1}$, $\boldsymbol{\eta}_{n+1}$, $\boldsymbol{\nu}_{n+1}^*$ and $\boldsymbol{\Lambda}_{n+1}^*$
        Evaluate the residuals of Eqs. (65d,65e,65f)
        Evaluate the iteration matrix of Eqs. (65d,65e,65f) with respect to $\mathbf{U}_{n+1}$ and $\boldsymbol{\nu}_{n+1}$
        Solve the resulting linearized problem and evaluate the corrections of $\mathbf{U}_{n+1}$ and $\boldsymbol{\nu}_{n+1}$
        Update the dependent variables $\mathbf{q}_{n+1}$ and $\boldsymbol{\nu}_{n+1}^*$
        Evaluate the residuals of Eqs. (65g,65h,65i)
        Evaluate the iteration matrix of Eqs. (65g,65h,65i) with respect to $\mathbf{W}_{n+1}$ and $\boldsymbol{\Lambda}_{n+1}$
        Solve the resulting linearized problem and evaluate the corrections of $\mathbf{W}_{n+1}$ and $\boldsymbol{\Lambda}_{n+1}$
        Update the dependent variables $\mathbf{v}_{n+1}$ and $\boldsymbol{\Lambda}_{n+1}^*$
    end for
end for

This nonlinear system can be solved using a semi-smooth Newton process, which can also be interpreted as an active set method [10, 22, 23, 24]. This method relies on iterations based on the linearized system with an update of the activation status at each iteration.

A simplification of the linearized system can be obtained if some coupling terms between equations are neglected in the iteration matrix that appears in the linearized problem. In this case, the solution of the full linearized problem within each iteration can be approximated by a sequence of three subproblems of size $n_q + n_g$ as described in Algorithm 1. A similar procedure was used in [12] and more implementation details can be found in that paper. In many practical cases, it turns out that this approximation of the iteration matrix does not significantly penalize the convergence of the process but significantly reduces the computational cost.

During the inner semismooth Newton iterations, the activation criteria are evaluated in non-converged states for which the equilibrium is not reached. The definition of these criteria based on the augmented Lagrange multipliers form is essential to ensure the robustness of the activation strategy and the convergence of the iterations towards the equilibrium state. Another important detail is that, even though the dependent variables are updated between the treatments of the different subsytems, the sets $\mathscr{A}$, $\mathscr{B}$ and $\mathscr{S}$ are evaluated only once at the begining of the global Newton iteration but are not updated between the treatments of the different subsystems.

4 Special case: smooth motion

The above algorithm is general and can deal with rigid and flexible multibody systems with bilateral constraints, unilateral contact conditions and impacts, involving velocity jumps and impulsive reaction forces. As a special case, it is also applicable to systems without unilateral constraints or with strictly closed unilateral constraints. In this case, no impact occurs and the dynamics evolves smoothly without velocity jumps or impulsive phenomena.

Even though we are interested in nonsmooth systems, the numerical performances of the method should also be investigated in the smooth phases of motion between impact phenomena. In this section, the equations of motion and the time integration algorithm are first particularized to smooth systems. Then, more usual DAE solvers for smooth systems will be reviewed and compared to the proposed algorithm.

If no impulsive contribution is present in Eqs. (21) and (23), we can write

$$d\mathbf{v} = \dot{\mathbf{v}} \, dt \tag{66}$$

$$d\mathbf{i} = \boldsymbol{\lambda} \, dt \tag{67}$$

and, if all active constraints remain closed, the dynamics can be represented by

$$\dot{\mathbf{q}} = \mathbf{v} \tag{68a}$$

$$\mathbf{M}(\mathbf{q}) \dot{\mathbf{v}} - \mathbf{g}_{\mathbf{q}}^T(\mathbf{q}) \boldsymbol{\lambda} = \mathbf{f}(\mathbf{q}, \mathbf{v}, t) \tag{68b}$$

$$\mathbf{g}(\mathbf{q}) = \mathbf{0} \tag{68c}$$

4.1 Special form of the proposed algorithm

For a smooth dynamic system without impact, Eq. (43) becomes

$$\mathbf{M}(\mathbf{q})\,\dot{\tilde{\mathbf{v}}} - \mathbf{g}_{\mathbf{q}}^{T}(\mathbf{q})\,\tilde{\boldsymbol{\lambda}} = \mathbf{f}(\mathbf{q},\mathbf{v},t) \tag{69a}$$

$$\mathbf{g}_{\mathbf{q}}(\mathbf{q})\,\dot{\tilde{\mathbf{v}}} + \mathbf{h}(\mathbf{q},\mathbf{v}) = \mathbf{0} \tag{69b}$$

$$\mathbf{M}(\mathbf{q})(\dot{\mathbf{q}} - \mathbf{v}) - \mathbf{g}_{\mathbf{q}}^{T}(\mathbf{q})\boldsymbol{\mu} = \mathbf{0} \tag{69c}$$

$$\mathbf{g}(\mathbf{q}) = \mathbf{0} \tag{69d}$$

$$\mathbf{M}(\mathbf{q})\,(\dot{\mathbf{v}} - \dot{\tilde{\mathbf{v}}}) - \mathbf{g}_{\mathbf{q}}^{T}(\mathbf{q})\,\boldsymbol{\xi} = \mathbf{0} \tag{69e}$$

$$\mathbf{g}_{\mathbf{q}}(\mathbf{q})\,\mathbf{v} = \mathbf{0} \tag{69f}$$

with $\boldsymbol{\xi} = \boldsymbol{\lambda} - \tilde{\boldsymbol{\lambda}}$. This equation has the structure of a stabilized index-1 DAE which combines the constraints at position, velocity and acceleration levels. One can check that any solution of Eq. (68) satisfies this formulation with $\boldsymbol{\mu} = \mathbf{0}$, $\boldsymbol{\xi} = \mathbf{0}$, $\boldsymbol{\lambda} = \tilde{\boldsymbol{\lambda}}$ and $\dot{\mathbf{v}} = \dot{\tilde{\mathbf{v}}}$. To the best of our knowledge, this form is not known in the multibody dynamics community. Nevertheless, it can be used in combination with various time integration schemes as index-1 DAEs are known to be less numerically sensitive than higher index systems.

The discrete form of Eq. (69) becomes

$$\mathbf{M}(\mathbf{q}_{n+1})\,\dot{\tilde{\mathbf{v}}}_{n+1} - \mathbf{g}_{\mathbf{q}}^{T}(\mathbf{q}_{n+1})\,\tilde{\boldsymbol{\lambda}}_{n+1} = \mathbf{f}(\mathbf{q}_{n+1},\mathbf{v}_{n+1},t_{n+1}) \tag{70a}$$

$$\mathbf{g}_{\mathbf{q}}(\mathbf{q}_{n+1})\,\dot{\tilde{\mathbf{v}}}_{n+1} + \mathbf{h}(\mathbf{q}_{n+1},\mathbf{v}_{n+1}) = \mathbf{0} \tag{70b}$$

$$\mathbf{M}(\mathbf{q}_{n+1})\mathbf{U}_{n+1} - \mathbf{g}_{\mathbf{q}}^{T}(\mathbf{q}_{n+1})\,\mathbf{v}_{n+1} = \mathbf{0} \tag{70c}$$

$$\mathbf{g}(\mathbf{q}_{n+1}) = \mathbf{0} \tag{70d}$$

$$\mathbf{M}(\mathbf{q}_{n+1})\,\mathbf{W}_{n+1} - \mathbf{g}_{\mathbf{q}}^{T}(\mathbf{q}_{n+1})\,\boldsymbol{\Lambda}_{n+1} = \mathbf{0} \tag{70e}$$

$$\mathbf{g}_{\mathbf{q}}(\mathbf{q}_{n+1})\,\mathbf{v}_{n+1} = \mathbf{0} \tag{70f}$$

that needs to be combined with the time integration formulae in Eq. (65j,65k,65l). In this case, the position correction $\mathbf{U}_{n+1}$ and the velocity jump $\mathbf{W}_{n+1}$ are only needed to compensate for the drift of the constraints at position and velocity levels that results from the time integration of the acceleration constraint at every time step. These corrections are thus expected to be small.

4.2 Other formulations for smooth systems with constraints at a single level

In multibody dynamics, one generally combines the kinematic equation and the dynamic equilibrium

$$\dot{\mathbf{q}} = \mathbf{v} \tag{71a}$$

$$\mathbf{M}(\mathbf{q})\,\dot{\mathbf{v}} - \mathbf{g}_{\mathbf{q}}^{T}\,\boldsymbol{\lambda} = \mathbf{f}(\mathbf{q},\mathbf{v},t) \tag{71b}$$

with the constraints either expressed at position level (index-3 formulation), velocity level (index-2 formulation) or acceleration level (index-1 formulation), or based on a linear combination according to the index-1 Baumgarte stabilization method as

follows

$$
\begin{cases}
\mathbf{g}(\mathbf{q}) = \mathbf{0} & \text{if position constraint} \\
\mathbf{g_q}(\mathbf{q})\,\mathbf{v} = \mathbf{0} & \text{if velocity constraint} \\
\mathbf{g_q}(\mathbf{q})\,\dot{\mathbf{v}} + \mathbf{h}(\mathbf{q},\mathbf{v}) = \mathbf{0} & \text{if acceleration constraint} \\
\mathbf{g_q}(\mathbf{q})\,\dot{\mathbf{v}} + \mathbf{h}(\mathbf{q},\mathbf{v}) + 2\,\alpha\,\mathbf{g_q}(\mathbf{q})\,\mathbf{v} + \beta^2\,\mathbf{g}(\mathbf{q}) = \mathbf{0} & \text{if Baumgarte form}
\end{cases}
$$

(71c)

These equations can be solved for given initial conditions $\mathbf{q}(0) = \mathbf{q}_0$ and $\mathbf{v}(0) = \mathbf{v}_0$. For the sake of consistency, these initial conditions need to verify the constraints at position and velocity levels.

The index-3 formulation is widely used for the simulation of multibody systems [8, 19]. Numerous theoretical results are available for implicit time integration schemes based on this formulation. For example, using the generalized-α time integration scheme, all solution components (position, velocities, accelerations and Lagrange multipliers) converge to the exact solution with second-order accuracy on finite time intervals. This result was first obtained for mechanical systems modelled as DAEs on a vector space [5] and later extended to systems with finite rotations variables and modelled as DAEs on a Lie group [7, 13]. In order to reduce the influence of numerical disturbances, a careful scaling strategy is recommended for the different equations and variables of the discrete system [11]. The hidden constraints at velocity and acceleration levels are not exactly satisfied but the constraint violation error stays in certain limits and decreases with the time step as fast as $\mathcal{O}(h^2)$ on finite time intervals. However, order reduction phenomena were pointed out in [7], which may affect the initial phase of a simulation by spurious transient numerical oscillations in the accelerations and Lagrange multipliers with $\mathcal{O}(h)$ amplitude. Also, the index-3 formulation cannot be directly extended to build time-stepping schemes for systems with unilateral constraints as it does not lend itself to the incorporation of the impact law.

The index-2 formulation based on the expression of the constraint at velocity level is equivalent to Eq. (36) in the special case of a smooth system without impact. It is thus particularly relevant for nonsmooth systems, as the impact law may be incorporated in the velocity constraint according to Moreau's sweeping process. In nonsmooth dynamics, the problem is usually integrated in time using a θ-method [2, 25, 27]. In this approach, the numerical solution is not forced to satisfy the constraint at position level so that drift-off phenomena can occur as a result of the accumulation of numerical integration errors.

The index-1 formulation based on the constraint at acceleration level is even less sensitive from a numerical point of view and can be solved using non-stiff time integration methods. However, it suffers from important drift-off phenomena at velocity and position levels [4]. These drift-off phenomena can be eliminated by the implementation of projection methods which bring the numerical solution back to the constraint manifold. The Baumgarte stabilization also enforces a single constraint but is formed as a weighted linear combination of the constraints at position, velocity and acceleration levels [9, 17]. In a strict sense, the resulting numerical solution does not satisfy any of these constraints individually. To the best of our knowl-

edge, these index-1 formulations have not been used in time-stepping schemes for unilaterally constrained systems with impacts and velocity jumps because the acceleration variable is not properly defined at the impact time. One of the original contribution of this chapter is to exploit the acceleration variable that results from the splitting procedure and is well-defined at any time for the formulation of the active constraints at acceleration level for nonsmooth mechanical systems.

4.3 Gear-Gupta-Leimkuhler formulation

The Gear-Gupta-Leimkuhler (GGL) formulation is another index reduction method that was initially developed for smooth DAEs and that simultaneously enforces the constraints at position and velocity levels [18]. It is based on the reformulation of the initial set of equations in index-2 form as

$$\dot{\mathbf{q}} - \mathbf{g}_{\mathbf{q}}^T \boldsymbol{\mu} = \mathbf{v} \tag{72a}$$

$$\mathbf{M}(\mathbf{q})\dot{\mathbf{v}} - \mathbf{g}_{\mathbf{q}}^T \boldsymbol{\lambda} = \mathbf{f}(\mathbf{q},\mathbf{v},t) \tag{72b}$$

$$\mathbf{g}(\mathbf{q}) = \mathbf{0} \tag{72c}$$

$$\mathbf{g}_{\mathbf{q}}(\mathbf{q})\mathbf{v} = \mathbf{0} \tag{72d}$$

One can check that any exact solution of the initial DAE (68) is also a solution of this set of equations with $\boldsymbol{\mu} = \mathbf{0}$.

As shown in [6, 7], this index-2 problem can be solved using the generalized-α method. In this chapter, the notations from these references are slightly adapted to match our previous developments. At time step $n+1$, the unknown variables $\mathbf{q}_{n+1}$, $\mathbf{v}_{n+1}$, $\dot{\mathbf{v}}_{n+1}$, $\boldsymbol{\lambda}_{n+1}$, $\mathbf{U}_n = h(\dot{\mathbf{q}}_n - \mathbf{v}_n)$ and $\boldsymbol{\nu}_n = h\boldsymbol{\mu}_n$ should thus satisfy

$$\mathbf{U}_n - \mathbf{g}_{\mathbf{q}}^T(\mathbf{q}_n)\boldsymbol{\nu}_n = \mathbf{0} \tag{73a}$$

$$\mathbf{M}(\mathbf{q}_{n+1})\dot{\mathbf{v}}_{n+1} - \mathbf{g}_{\mathbf{q}}^T(\mathbf{q}_{n+1})\boldsymbol{\lambda}_{n+1} = \mathbf{f}(\mathbf{q}_{n+1},\mathbf{v}_{n+1},t_{n+1}) \tag{73b}$$

$$\mathbf{g}(\mathbf{q}_{n+1}) = \mathbf{0} \tag{73c}$$

$$\mathbf{g}_{\mathbf{q}}(\mathbf{q}_{n+1})\mathbf{v}_{n+1} = \mathbf{0} \tag{73d}$$

together with the integration formula

$$\mathbf{q}_{n+1} = \mathbf{q}_n + h\mathbf{v}_n + h^2(0.5 - \beta)\mathbf{a}_n + h^2\beta\mathbf{a}_{n+1} + \mathbf{U}_n \tag{73e}$$

$$\mathbf{v}_{n+1} = \mathbf{v}_n + h(1 - \gamma)\mathbf{a}_n + h\gamma\mathbf{a}_{n+1} \tag{73f}$$

$$(1 - \alpha_m)\mathbf{a}_{n+1} + \alpha_m\mathbf{a}_n = (1 - \alpha_f)\dot{\mathbf{v}}_{n+1} + \alpha_f\dot{\mathbf{v}}_n \tag{73g}$$

This method leads to a numerical solution which simultaneously satisfies the constraints at position and velocity levels. Unlike in the analytical solution, the multiplier $\boldsymbol{\nu}_n$ of the numerical solution is not exactly $\mathbf{0}$, with the consequence that $\mathbf{U}_n \neq \mathbf{v}_n$. Compared to the index-3 formulation, this method is less numerically sen-

sitive and is not prone to the order reduction phenomenon mentioned in the previous
section [7].

In order to highlight the connection with the nonsmooth algorithm discussed in
this chapter and in [12], the method can be slightly adapted as

$$\mathbf{M}(\mathbf{q}_{n+1})\mathbf{U}_{n+1} - \mathbf{g}_{\mathbf{q}}^T(\mathbf{q}_{n+1})\,\boldsymbol{\nu}_{n+1} = \mathbf{0} \tag{74a}$$

$$\mathbf{M}(\mathbf{q}_{n+1})\dot{\mathbf{v}}_{n+1} - \mathbf{g}_{\mathbf{q}}^T(\mathbf{q}_{n+1})\,\boldsymbol{\lambda}_{n+1} = \mathbf{f}(\mathbf{q}_{n+1},\mathbf{v}_{n+1},t_{n+1}) \tag{74b}$$

$$\mathbf{g}(\mathbf{q}_{n+1}) = \mathbf{0} \tag{74c}$$

$$\mathbf{g}_{\mathbf{q}}(\mathbf{q}_{n+1})\mathbf{v}_{n+1} = \mathbf{0} \tag{74d}$$

with the time integration formulae

$$\mathbf{q}_{n+1} = \mathbf{q}_n + h\mathbf{v}_n + h^2(0.5 - \beta)\mathbf{a}_n + h^2\beta\mathbf{a}_{n+1} + \mathbf{U}_{n+1} \tag{74e}$$

$$\mathbf{v}_{n+1} = \mathbf{v}_n + h(1 - \gamma)\mathbf{a}_n + h\gamma\mathbf{a}_{n+1} \tag{74f}$$

$$(1 - \alpha_m)\mathbf{a}_{n+1} + \alpha_m\mathbf{a}_n = (1 - \alpha_f)\dot{\mathbf{v}}_{n+1} + \alpha_f\dot{\mathbf{v}}_n \tag{74g}$$

Two changes can be observed between Eq. (73) and Eq. (74). Firstly, the mass matrix
$\mathbf{M}$ now appears in Eq. (74a). Secondly, the position correction $\mathbf{U}_{n+1}$ that appears in
the position update Eq. (74e) is evaluated at time step $n+1$ (and not at time step n
as in Eq. (73e)).

Various investigations addressed the extension of the GGL formulation for non-
smooth systems [1, 12, 36]. Also, the formulation presented in Section 4.1 can be
interpreted as a recursive application of the GGL method so that the constraints at
acceleration level are also incorporated.

4.4 Emulation of post-impact conditions

If an impact is followed by a free-flight phase on a finite time interval, the post-
impact numerical solution will be affected by disturbances which will propagate dy-
namically in the free-flight phase. An important question is thus to characterize the
behaviour of the algorithm for smooth mechanical systems with a particular focus
on the sensitivity to disturbances induced by impulsive phenomena and constraint
activations. This section shows that the behaviour of the nonsmooth generalized-α
method in the post-impact phase can be investigated based on the underlying smooth
system with disturbed initial conditions.

Let us consider a nonsmooth system and imagine that an isolated impact occurs
in the time interval $[t_{n-1}, t_n)$ but that no other nonsmooth phenomenon arises for
$t > t_n$. Over the time interval $[t_{n-1}, t_n)$, the velocity is discontinuous but the dis-
placement remains continuous in time. If the system is simulated either using the
method described in [12] or the method proposed in this paper, the numerical so-
lution at t_{n+1} only depends on $\mathbf{q}_n$, $\mathbf{v}_n$, $\dot{\mathbf{v}}_n$ and $\mathbf{a}_n$ (we do not need to evaluate $\boldsymbol{\eta}_{n+1}$,
$\boldsymbol{\Lambda}_{n+1}^*$ and $\boldsymbol{\nu}_{n+1}^*$ as the constraint status is assumed to be known for $t > t_n$). Let us

analyze the consistency of these variables ($\mathbf{q}_n$, $\mathbf{v}_n$, $\dot{\tilde{\mathbf{v}}}_n$, $\mathbf{a}_n$) with respect to the bilateral constraints in the post-impact phase.

The positions $\mathbf{q}_n$ and velocities $\mathbf{v}_n$ are, by construction, consistent with the bilateral constraints at position and velocity levels. Therefore, at position and velocity levels, the discontinuity leads to new and consistent initial conditions and erases the pre-impact time history.

As the velocity is discontinuous, the acceleration $\dot{\tilde{\mathbf{v}}}$ defined according to our splitting method also undergoes an $\mathcal{O}(1)$ discontinuity over the time interval $[t_{n-1}, t_n)$. At t_n, consistent values of the acceleration $\dot{\tilde{\mathbf{v}}}_n$ and of the shifted value $\mathbf{a}_n$ could be computed from Eq. (38) based on the value of $\mathbf{q}_n$ and $\mathbf{v}_n$, using a similar technique as for the definition of the initial conditions. The results would thus be consistent and completely independent of the values of the pre-impact solution. This strategy would be interpreted as a reinitialization of the time integration procedure after the impact.

However, the method described in [12] and the method proposed here do not rely on a reinitialization procedure, as we do not want to perform specific treatments every time an impact occurs. Instead, the smooth acceleration is integrated over the impact according to the generalized-α method as if no discontinuity were present. Therefore, the pre-impact acceleration history influences the post-impact numerical solution as follows.

- In the method described in [12], for given values of $\mathbf{q}_n$ and $\mathbf{v}_n$, the values of $\dot{\tilde{\mathbf{v}}}_n$ and $\mathbf{a}_n$ still depend on the pre-impact values $\dot{\tilde{\mathbf{v}}}_{n-1}$, $\mathbf{a}_{n-1}$ and $\mathbf{v}_{n-1}$.
- In the algorithm proposed here the value of $\dot{\tilde{\mathbf{v}}}_n$ is defined as an algebraic function of $\mathbf{q}_n$ and $\mathbf{v}_n$ and is thus independent of the pre-impact solution, but the value of $\mathbf{a}_n$ still depends on the pre-impact values $\dot{\tilde{\mathbf{v}}}_{n-1}$ and $\mathbf{a}_{n-1}$ (see Eq. (65l)).

Compared to a correct reinitialization of the acceleration variables solely based on the post-impact state, the pre-impact solution influences the values $\mathbf{a}_n$ and possibly $\dot{\tilde{\mathbf{v}}}_n$ in both algorithms, leading to $\mathcal{O}(1)$ disturbances. As a consequence, $\mathbf{a}_n$ and possibly $\dot{\tilde{\mathbf{v}}}_n$ may violate the constraint at acceleration level with $\mathcal{O}(1)$ errors. Thus, the post-impact numerical solution can be emulated by a simulation of the underlying smooth system for $t > t_n$ if the initial accelerations $\dot{\tilde{\mathbf{v}}}_n$ and $\mathbf{a}_n$ are modified with $\mathcal{O}(1)$ disturbances.

This situation is also representative of the transition of a unilateral constraint from an open to a closed status in $\mathscr{S}$ over the time interval $[t_{n-1}, t_n)$. Indeed, in this case, the position $\mathbf{q}_n$ and velocity $\mathbf{v}_n$ satisfy the new constraint at position and velocity levels, but the acceleration $\dot{\tilde{\mathbf{v}}}_n$ and the shifted variable $\mathbf{a}_n$ do not necessarily satisfy the new constraint at acceleration level.

5 Application to a smooth system

The properties of the proposed method are first investigated in the context of the numerical solution of smooth DAEs. The classical example of a pendulum modelled

as a constrained mechanical system serves for the comparison. Numerical methods derived from the generalized-α method using four different formulations of the equations of motion are compared:

- the index-3 formulation with the constraints at position level only, referred as the "P-constrained" method;
- the index-2 formulation with the constraints at velocity level only, referred as the "V-constrained" method;
- the index-2 Gear-Gupta-Leimkuhler formulation with the constraints at position and velocity levels, referred as the "PV-constrained" method;
- the proposed index-1 formulation with the constraints imposed simultaneously at position, velocity and acceleration levels, referred as the "PVA-constrained" method.

5.1 Problem description
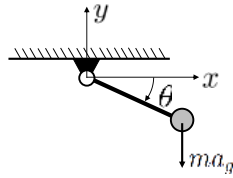
Fig. 1 Pendulum.

Let us analyse the transient response of the pendulum depicted in Fig. 1. In order to study the behaviour of the algorithm in the presence of constraints, a set of 3 absolute but redundant coordinates is chosen $\mathbf{q} = [x \, y \, \theta]^T$ where x and y are the coordinates of the center of mass and θ is the angle of the pendulum. These coordinates have to satisfy 2 bilateral constraints

$$g^1(\mathbf{q}) \equiv x - L\cos\theta = 0 \tag{75}$$
$$g^2(\mathbf{q}) \equiv y - L\sin\theta = 0 \tag{76}$$

The physical parameters of the system are selected as: length of the pendulum $L = 1\,\text{m}$, mass $m = 1\,\text{kg}$, moment of inertia $J = 0.1\,\text{kg m}^2$, and gravity acceleration along the y-axis $a_g = 10\,\text{rad/s}^2$. The initial conditions at position and velocity levels are defined as $\theta_0 = \pi/6\,\text{rad}$ and $\dot{\theta}_0 = 10\,\text{rad/s}$. The numerical parameters of the numerical solvers are selected as $h = 2.10^{-3}\,\text{s}$, $\rho_\infty = 0.9$.
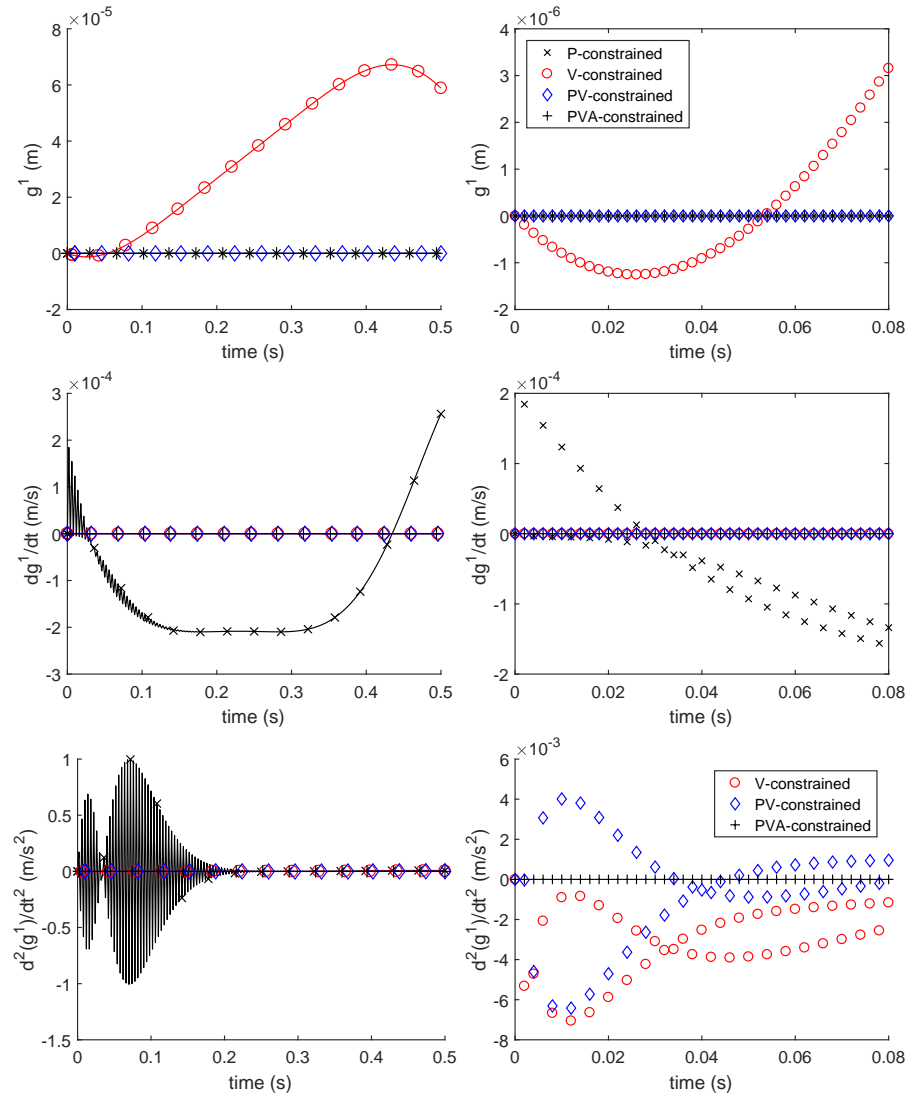
Fig. 2 Position (top), velocity (middle) and acceleration (bottom) constraints in the pendulum example - left: full time interval, right: zoom on the initial phase. In the bottom-right plot, the solution of the index-3 problem with the position constraint is not represented for the sake of readibility.

5.2 Results based on consistent initial conditions

Consistent initial positions $\mathbf{q}$ and velocities $\mathbf{v}$ are established from the initial value θ_0 and $\dot{\theta}_0$. The initial acceleration $\dot{\mathbf{v}}$ is obtained by solving Eq. (38) at time t_0 and the shifted acceleration is initialized as $\mathbf{a}_0 = \dot{\mathbf{v}}_0$. The results are presented in Fig. 2. On certain graphs, high numerical oscillations are observed at the frequency of the step size, which means that the variable under study jumps between a low to a high value at each step. For the sake of readability, when zooming on these phenomena, only the values at the successive time steps are represented by markers but the interpolating line between the time steps is not necessarily displayed.

In the index-3 solution based on the sole position constraint, spurious high frequency oscillations of the constraint at velocity and acceleration levels are observed in the initial phase. After a transient phase, these high-frequency oscillations are damped out and the hidden constraints do not converge to zero but evolve in a continuous manner. The amplitude of the transient high-frequency oscillations of the acceleration constraint is particularly large and it can be shown that it decreases only as $\mathscr{O}(h)$ when the time step is decreased, which reflects the presence of an order reduction phenomenon, as discussed in Sect. 4.2.

In the index-2 solution based on the sole velocity constraint, a constraint drift is observed at position level which increases as time goes by. Spurious high-frequency oscillations are observed at acceleration level, but it can be shown that their amplitude is quite limited and decreases as fast as $\mathscr{O}(h^2)$ when the time step decreases, i.e., there is no order reduction phenomenon in this case. After a transient phase, the spurious oscillations disappear and the acceleration constraint evolves in a continuous manner.

In the index-2 GGL solution, which enforces the constraints at position and velocity levels, the constraints are indeed satisfied up to machine precision at position and velocity levels. At acceleration level, the behaviour is similar as for the other index-2 solution discussed in the previous paragraph.

In the proposed index-1 solution, the results confirm that the constraints are satisfied up to machine precision at the three levels (position, velocity and acceleration).

5.3 Results based on post-impact initial conditions

In order to emulate the disturbances induced by an impact on the post-impact numerical solution, the simulation of the rigid pendulum is run using disturbed initial accelerations such that the constraint is not satisfied at acceleration level.

Figure 3 presents the simulation results for the pendulum when the acceleration and shifted acceleration are initialized as $\dot{\mathbf{v}}_0 = \mathbf{a}_0 = \mathbf{0}$. Large spurious oscillations of the acceleration constraint and Lagrange multiplier are observed for all algorithms excepted for the proposed method which enforces the constraints at position, velocity and acceleration levels. Thus, the proposed method appears much less sensitive to the disturbances induced by impact phenomena.
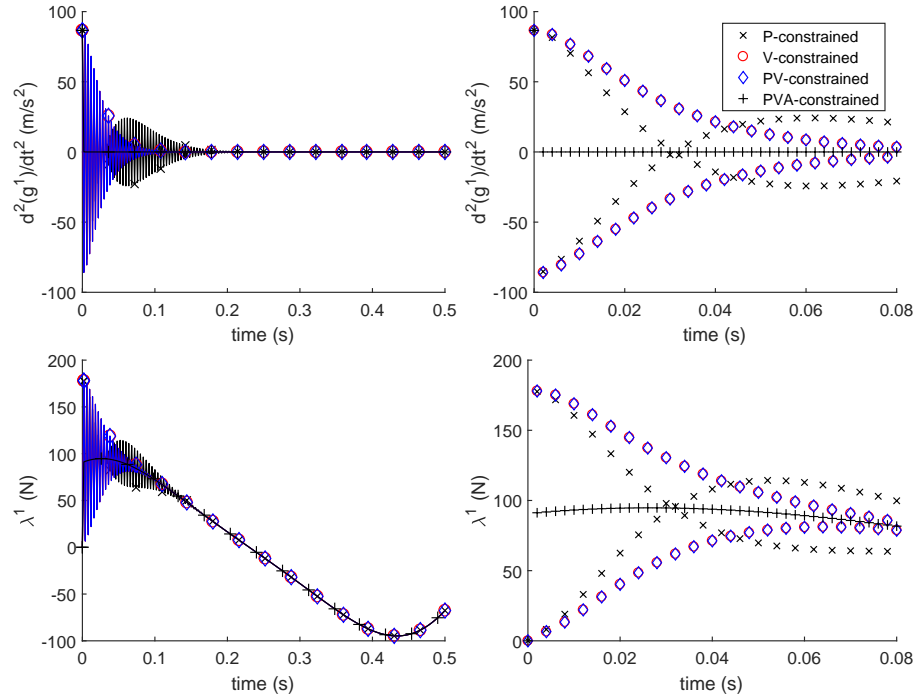
Fig. 3 Acceleration constraint (top) and Lagrange multiplier (bottom) in the pendulum example with post-impact initial conditions (left: full time interval, right: zoom on the initial phase).

6 Application to nonsmooth systems

In this section, three numerical examples are used to compare two algorithms for nonsmooth dynamic systems

- The algorithm described in [12] in which the constraint on the smooth motion only includes the bilateral constraints which are imposed at velocity level;
- The algorithm proposed here in which the constraint on the smooth motion includes the bilateral constraints as well as the active unilateral constraints both imposed at acceleration level.

These two algorithms will be respectively called the "PVV-constrained" method and the "PVA-constrained" method in the following. In both algorithms, the smooth motion is integrated using the generalized-α time integration formula.

The first example is a bouncing rigid pendulum, the second example is a bouncing elastic pendulum modelled as a geometrically exact beam and the last example is the horizontal impact of an elastic bar. These three examples served also as a support for the analysis of several algorithms for nonsmooth systems in [12, 14].

Here, these examples are exploited to explore the properties the PVA-constrained algorithm which is a novel contribution of this chapter.

6.1 Bouncing rigid pendulum
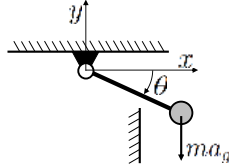
Fig. 4 Bouncing pendulum.

We consider the same pendulum as described in Sect. 5.1 but, as shown in Fig. 4, a unilateral constraint restricts the motion of its center of mass as

$$g^3(\mathbf{q}) \equiv x - x_{\min} \geq 0 \tag{77}$$

with $x_{\min} = \sqrt{2}/2$ m. The initial conditions are $\theta_0 = \pi/12$ rad and $\dot{\theta}_0 = 0$ rad/s. Consistent initial conditions are then defined for $\mathbf{q}$, $\mathbf{v}$, $\dot{\mathbf{v}}$ and $\mathbf{a}$. The time step and the spectral radius are selected as $h = 1.10^{-3}$ s and $\rho_\infty = 0.9$.
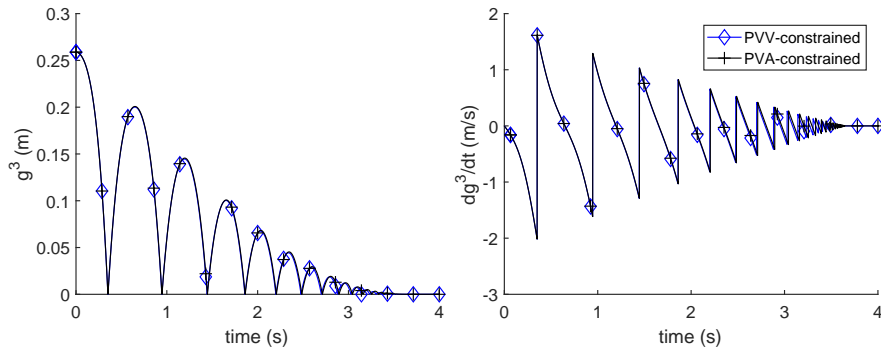
Fig. 5 Unilateral constraint in the bouncing rigid pendulum example (left: position level, right: velocity level).

The evolution of the gap distance $g^3(\mathbf{q})$ during the motion is shown in Figure 5. The pendulum bounces several time against the hurdle and, at the end of the trajec-
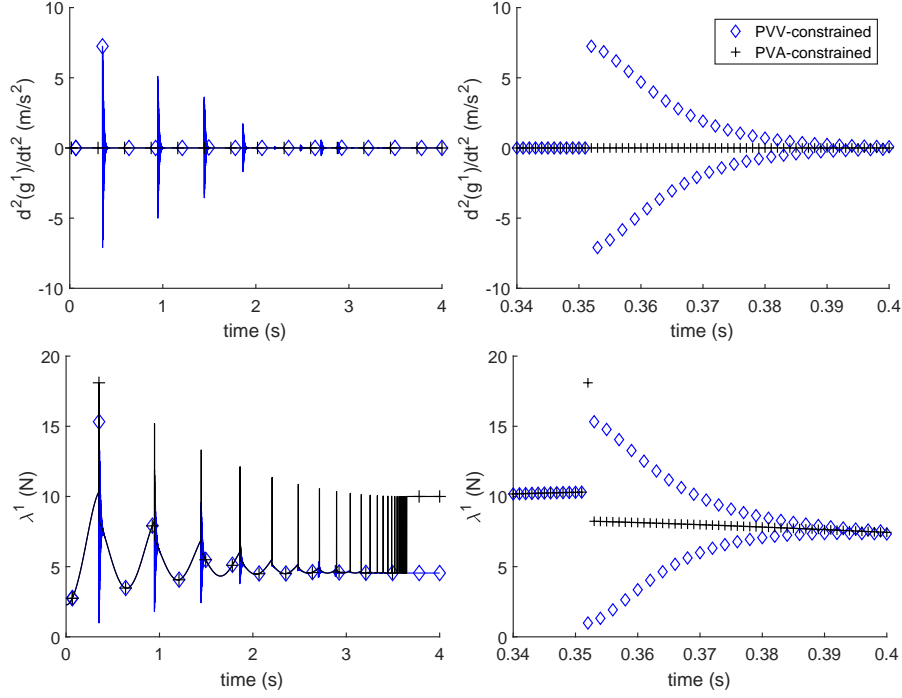
Fig. 6 Bouncing rigid pendulum: bilateral constraint at acceleration level (top) and Lagrange multipliers $\tilde{\boldsymbol{\lambda}}$ (bottom) - left: full time interval, right: zoom on the first impact.

tory, the system gets stabilized in the closed contact configuration after an accumulation phenomenon.

The evolution of the bilateral constraint at acceleration level (Fig. 6) reveals significant numerical oscillations after each impact in the PVV-constrained algorithm. In contrast, the solution obtained using the PVA-constrained method exactly satisfies the acceleration constraints without any such oscillations. In the same figure, similar oscillations are observed in the smooth bilateral multiplier $\tilde{\lambda}^1$ evaluated using the PVV-constrained method. In the PVA-constrained method, a discontinuity occurs at each impact but no oscillation is visible.

At the end of the trajectory, the nonsmooth phenomena disappear and the total horizontal reaction force in the rigid body becomes constant and can simply be estimated as $\tilde{\lambda}^1 + \Lambda^1/h$. Considering Figs. 6 (bottom-left) and 7 (right), the same total reaction force is obtained in the two methods at the end of the trajectory but the value of the relative impulse Λ^1 is equal to zero in the proposed algorithm. Indeed, in this smooth part of the trajectory, the smooth equation captures the total motion and, in this case, the corrections at position and velocity levels $\mathbf{W}$ and $\mathbf{U}$ tend to zero for the PVA-constrained algorithm.
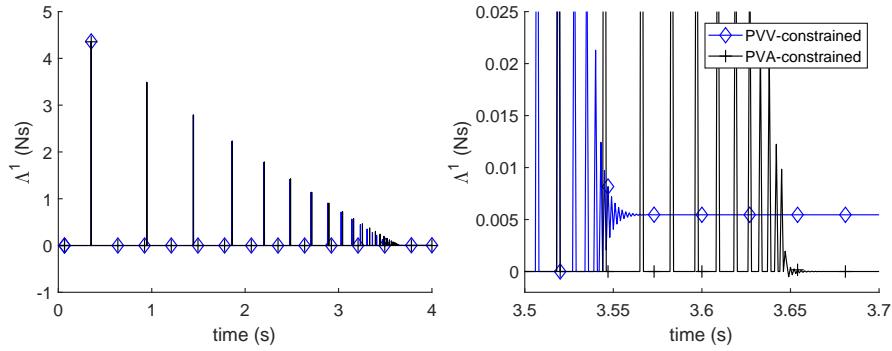
Fig. 7 Lagrange multiplier $\tilde{\Lambda}$ of the bilateral constraint in the bouncing pendulum example (left: full time interval, right: zoom on the end phase).
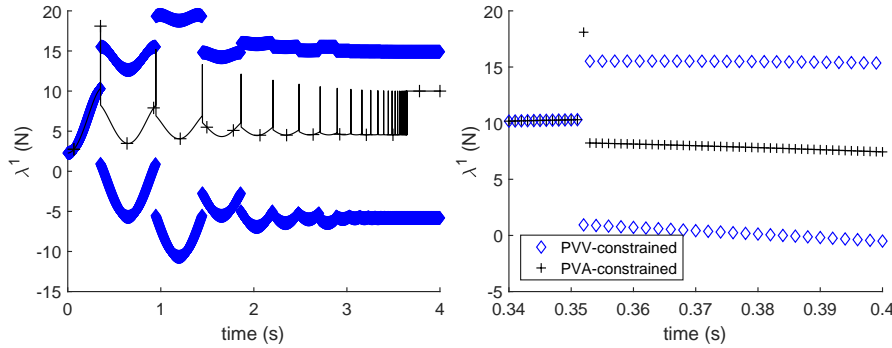

Fig. 8 No numerical damping - Lagrange multiplier $\tilde{\lambda}$ of the bilateral constraint in the bouncing pendulum example (left: full time interval, right: zoom on the first impact).

In the transient phase before the unilateral constraint gets closed, the relative impulse Λ^1 can take negative values in the PVA-constrained method as the complementarity condition is not applied to Λ^1 but to Λ^{*1}.

The PVA-constrained method generally brings less numerical dissipation since the reaction forces are better integrated. This is in agreement with the observation of a later stabilization of the system in the closed contact state in Fig. 7.

Finally, the results in Fig. 8 were obtained using a spectral radius $\rho_\infty = 1$, i.e., without any numerical dissipation. The PVA-constrained method still gives the expected results without any spurious numerical oscillation, whereas the Lagrange multiplier obtained from the PVV-constrained method undergoes strong oscillations after the first impact which never disappear from the solution.

In summary, this example has shown that both algorithms give a satisfactory numerical solutions which exactly satisfies the bilateral and unilateral constraints at position and velocity levels. Their comparison reveals (i) that imposing the con-

straints at acceleration level improves the handling of the bilateral constraints after the impact phenomena and alleviates the need to introduce numerical dissipation in the time integration scheme in this example, (ii) that the unilateral constraint can be activated at acceleration level in the smooth motion. During the free flight mode or the closed constraint mode, the smooth motion then captures the full motion which is thus integrated with second-order accuracy without any spurious oscillations.

6.2 Bouncing flexible pendulum
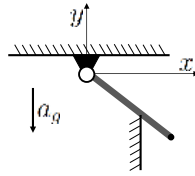
Fig. 9 Bouncing elastic pendulum.

In this example shown in Fig. 9, a flexible pendulum modelled as an elastic beam hits an obstacle. The beam is modelled according to the geometrically exact beam theory and discretized into nonlinear finite elements [19]. Thus, this example highlights nonlinear interactions between the beam and the non-penetration constraint at the contact point.

The contact condition is modelled as a unilateral constraint applied at the tip node of the beam mesh

$$g^1(\mathbf{q}) \equiv x_{\text{tip}} - x_{\text{min}} \geq 0 \tag{78}$$

There is no bilateral constraint in this example. The properties of the beam are: undeformed length $L = 1$ m, cross section area $A = 10^{-4}$ m^2, cross section inertia $I = 8.33 \, 10^{-10}$ m^4, shear section area $A_s = (5/6)A$, Young modulus $E = 2.1 \, 10^{11}$ N/m^2, density $\rho = 7800$ kg/m^3, Poisson coefficient $\nu = 0.3$. At the initial time, the beam is horizontal with zero velocity. The unilateral constraint is defined as $x_{\text{min}} = L\sqrt{2}/2$.

The beam is modelled using four finite elements. The time step is $h = 5.\,10^{-6}$ s and the spectral radius is $\rho_\infty = 0.8$. A restitution coefficient is included in the formulation of the impact law and its value is defined as $e = 0$.

In the PVV-constrained method, the unilateral constraint is never activated at acceleration level in the definition of the smooth motion. As there is no bilateral constraint in this case, the smooth motion is thus fully unconstrained. In the PVA-constrained method, the unilateral constraint at acceleration level gets activated and deactivated in a dynamic manner, so that the constraint reaction force brings some stronger disturbances on the smooth motion.
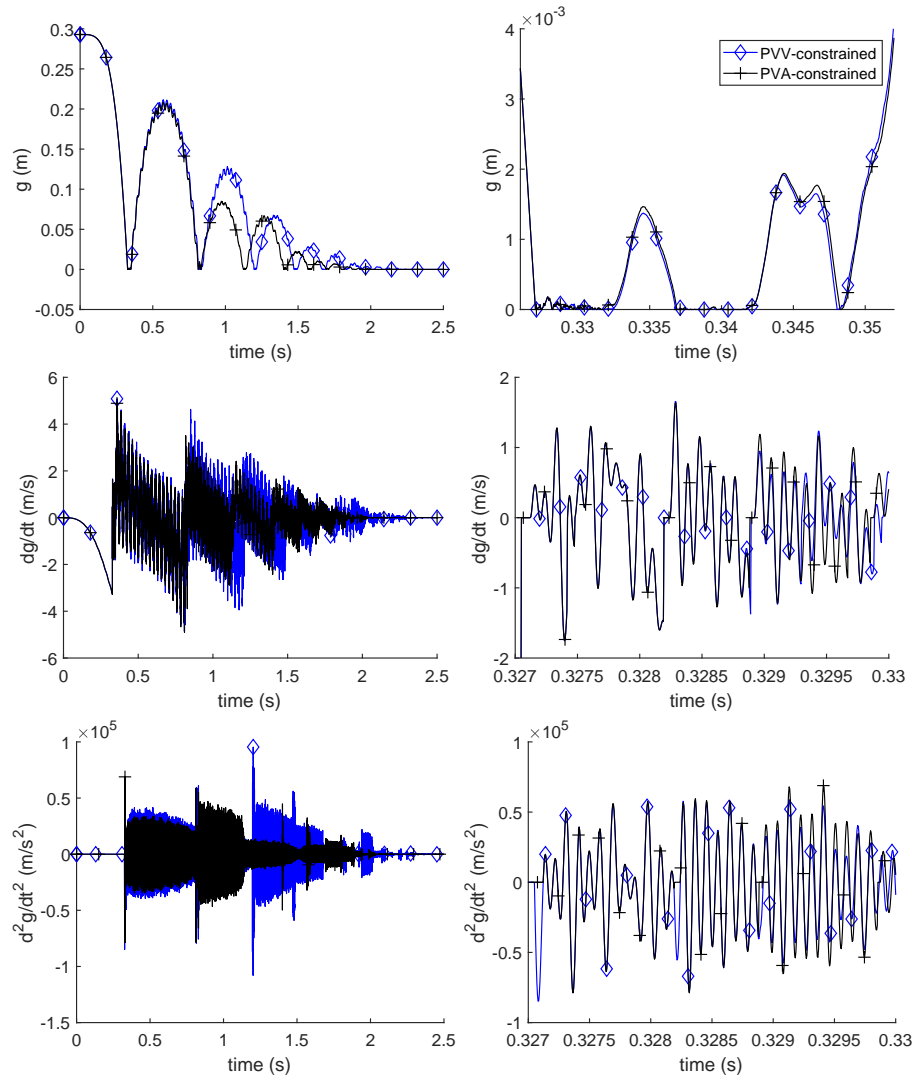
Fig. 10 Bouncing flexible pendulum: unilateral constraint at position (top), velocity (middle) and acceleration levels (bottom) - left: full time interval, right: zoom on the first contact phase (the zoom interval is different for the position constraint).

As the step-size h is quite small, the mean number of Newton iterations at each time step is very close to one for both algorithms.

The constraints at position, velocity and acceleration levels are depicted in Fig. 10. The numerical response is characterized by rather complex dynamic phenomena. The first contact phase is characterized by a finite duration on the interval [0.327,0.348] s. However, the contact at position, velocity and acceleration levels do not stay permanently activated over this time interval but enter and leave the system in an intermittent manner. The zooms on the initial contact phase indicate a good agreement between the two algorithms at position, velocity and acceleration level. The solutions tend to diverge later on as the problem is particularly sensitive. One also observes the activation of the constraint at acceleration level for some time intervals in the PVA-constrained method, whereas this constraint is never activated in the PVV-constrained method.
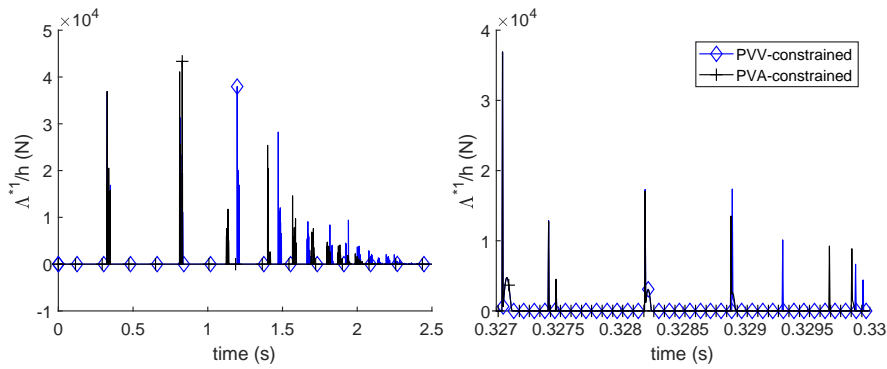

Fig. 11 Reaction force in the bouncing pendulum example (left: full time interval, right: zoom on the first contact phase).

The reaction forces at the contact point are represented in Fig. 11. During the first contact phase, one observes a collection of rather close impulses.

In Fig. 12, the energy decays monotonously during the motion. During the first contact phase, the energy decays progressively according to a kind of staircase function. One also observe the faster energy decay of the PVV-constrained method which can be attributed to the higher level of numerical dissipation in this scheme.

In summary, the bouncing elastic pendulum example shows the ability of both algorithms to study the dynamics a geometrically nonlinear beam with a unilateral constraint. Both methods show similar numerical performances in this case which involves high frequency activation and deactivation phenomena during the contact phases.
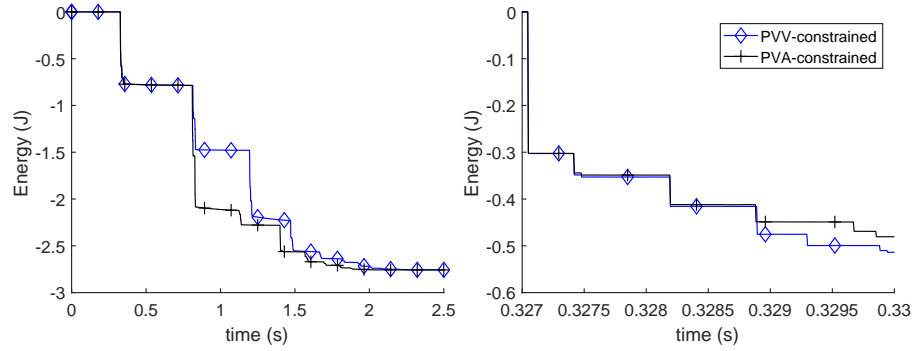
Fig. 12 Constraint at velocity level and energy in the bouncing pendulum example (left: full time interval, right: zoom on the first contact phase).
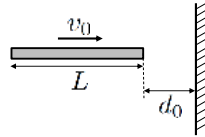
6.3 Horizontal impact of an elastic bar

Fig. 13 Horizontal impact of an elastic bar.

The horizontal impact of an elastic bar as shown in Fig. 13 is now considered. The problem was described in [16] and has an analytical solution. According to this analytical solution, the contact stays closed for a period of $\Delta t = 2L\sqrt{\rho/E}$ and the energy is conserved. The contact force remains finite so there is no impact even if the velocity undergoes a discontinuity at the contact point when the contact closes.

In our finite element model, a restitution coefficient e is needed at the level of the impact law. This coefficient has no physical meaning and simply represents the energy dissipation in the last element of the mesh. In order to be able to represent the instantaneous closing of the unilateral constraint, we propose to choose $e = 0$.

The physical parameters are defined as in [16]: Young modulus $E = 900\,\text{N/m}^2$, density $\rho = 1\,\text{kg/m}^3$, undeformed length $L = 10\,\text{m}$, initial distance from the obstacle $d_0 = 5\,\text{m}$, initial velocity $v_0 = 10\,\text{m/s}$. With these data, the closed contact period is $\Delta t = 2/3\,\text{s}$. The bar is discretized using 200 finite elements, the time step is taken as $h = 2.10^{-3}\,\text{s}$, and the spectral radius of the generalized-α time integrator is chosen as $\rho_\infty = 0.8$.

The results are presented in Figs 14, 15 and 16. The two algorithms give very close results. The main difference is found in the mean number of Newton itera-
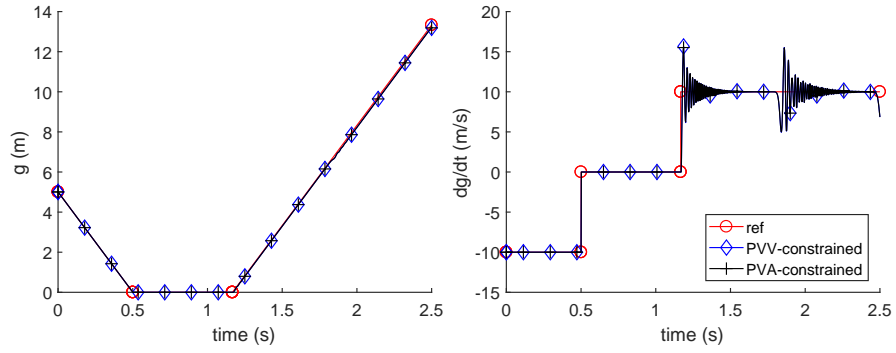
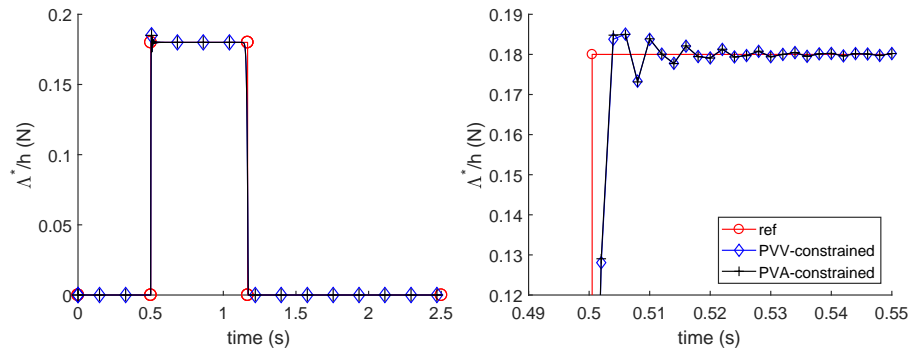**Fig. 14** Unilateral constraint in the bar impact example (left: position level, right: velocity level).

Fig. 15 Reaction force Λ^*/h in the bar impact example (left: full time interval, right: zoom on the post-impact phase).
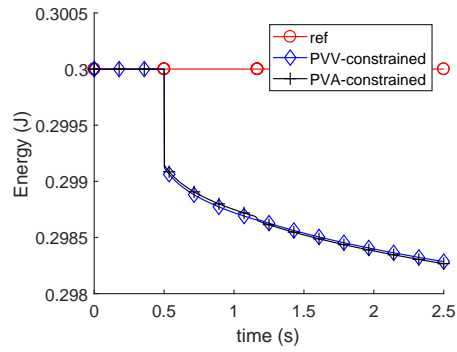

Fig. 16 Energy in the bar impact example.

tions at each time step. In the PVV-constrained method, we have 2.94 iterations per time step (about 10 iterations per step during the contact phase) whereas in the PVA-constrained method only 0.80 iterations are needed in average. The explanation is that the PVV-constrained method completely disregards the unilateral constraint when evaluating the smooth motion. Therefore, the physical solution is rather far from the smooth solution, the position and velocity corrections **U** and **W** are quite significant and more iterations are needed to solve the coupled problem.

This example shows that the two methods provide relevant numerical solutions of unilaterally constrained structure with closed contacts. Once again, the constraints at position and velocity levels are exactly satisfied by the numerical solution. This study also reveals the superiority of the PVA-constrained algorithm for flexible systems when some unilateral constraints stay closed during rather long time intervals.

7 Conclusion

The nonsmooth generalized-α method was developed for the analysis of flexible multibody systems with contact conditions and impact phenomena. It relies on a splitting of the total motion into smooth (non-impulsive) and nonsmooth (impulsive) contributions. A second-order time integration scheme is then used for the smooth contributions whereas a first-order scheme is used for the consistent integration of impulsive contributions. Compared to the classical Moreau-Jean method, this method leads to qualitatively better numerical solutions with less numerical dissipation.

This chapter addresses the formulation of the constraints that appear in the definition of the smooth motion and which can have a deep impact on the numerical properties of the scheme. We propose to impose all active constraints at acceleration levels on the smooth part of the motion, while the total motion satisfies simultaneously the constraints at position and velocity levels. Some advantages of this formulation are the elimination of spurious numerical oscillations of the constraints that generally occur after an impact and the possibility to account for the contributions of the unilateral constraints to the smooth motion. When the contact remains closed, the integration of the contact forces is performed with a higher accuracy, which comes with a reduced level of numerical dissipation and the convergence of the approximated Newton iterations is accelerated as the amplitudes of the nonsmooth corrections are reduced. These properties were demonstrated in several numerical examples of smooth and nonsmooth mechanical systems. It is remarkable that, in rigid-body examples, the constraints and the overall numerical solution are inherently stabilized (in the sense that no spurious numerical oscillation is observed) even if no numerical dissipation is introduced at the level of the generalized-α time integrator.

Some key elements of the method can also be summarized. Firstly, the proposed splitting strategy leads to a definition of the acceleration variable $\dot{\mathbf{v}}$ as an algebraic function of the physical position and velocity at the current time, which permits

the dynamic activation and deactivation of unilateral constraints in a very simple manner. The acceleration $\dot{\tilde{\mathbf{v}}}$ represents the standard acceleration for almost every time but it excludes impulsive contributions at the impact instants. Even though this acceleration is discontinuous, the position and velocity of the smooth trajectory are continuous even in the presence of impacts. The definition of the activation criteria for the unilateral constraints at position, velocity and acceleration levels is particularly critical for the robustness of the algorithm. The proposed criteria rely on the definition of augmented Lagrange multipliers at position, velocity and acceleration levels and can thus be used in a reliable way within the Newton semismooth iterations even if the solution is not yet converged.

As a perspective, the present algorithm could be tested for more complex examples with a larger number of bodies and contact conditions. The extension to frictional contact conditions could also be investigated.

References

1. Acary, V.: Projected event-capturing time-stepping schemes for nonsmooth mechanical systems with unilateral contact and Coulomb's friction. Computer Methods in Applied Mechanics and Engineering **256**(10), 224–250 (2013)
2. Acary, V., Brogliato, B.: Numerical methods for nonsmooth dynamical systems - Applications in Mechanics and Electronics, *Lecture Notes in Applied and Computational Mechanics*, vol. 35. Springer-Verlag, Berlin (2008)
3. Alart, P., Curnier, A.: A mixed formulation for frictional contact problems prone to Newton like solution methods. Computer Methods in Applied Mechanics and Engineering **92**, 353–375 (1991)
4. Arnold, M.: Numerical methods for simulation in applied dynamics. In: W. Schiehlen, M. Arnold (eds.) Simulation Techniques in Applied Dynamics - CISM Lecture Notes, Volume 507, pp. 191–246. Springer-Verlag, Wien (2008)
5. Arnold, M., Brüls, O.: Convergence of the generalized-α scheme for constrained mechanical systems. Multibody System Dynamics **18**(2), 185–202 (2007)
6. Arnold, M., Brüls, O., Cardona, A.: Convergence analysis of generalized-α Lie group integrators for constrained systems. In: Proceedings of Multibody Dynamics ECCOMAS Thematic Conference. Brussels (2011)
7. Arnold, M., Brüls, O., Cardona, A.: Error analysis of generalized-α Lie group time integration methods for constrained mechanical systems. Numerische Mathematik **129**, 149–179 (2015)
8. Bauchau, O.: Flexible multibody dynamics. Springer, Dordrecht (2011)
9. Baumgarte, J.: Stabilization of constraints and integrals of motion in dynamical systems. Computer Methods in Applied Mechanics and Engineering **1**, 1–16 (1972)
10. Ben Gharbia, I., Gilbert, J.: Nonconvergence of the plain Newton-min algorithm for linear complementarity problems with a P-matrix. Mathematical Programming, Series A **134**, 349–364 (2012)
11. Bottasso, C., Bauchau, O., Cardona, A.: Time-step-size-independent conditioning and sensitivity to perturbations in the numerical solution of index three differential algebraic equations. SIAM Journal on Scientific Computing **29**(1), 397–414 (2007)
12. Brüls, O., Acary, V., Cardona, A.: Simultaneous enforcement of constraints at position and velocity levels in the nonsmooth generalized-α scheme. Computer Methods in Applied Mechanics and Engineering **281**, 131–161 (2014)
13. Brüls, O., Cardona, A., Arnold, M.: Lie group generalized-α time integration of constrained flexible multibody systems. Mechanism and Machine Theory **48**, 121–137 (2012)

14. Chen, Q.z., Acary, V., Virlez, G., Brüls, O.: A nonsmooth generalized-α scheme for flexible multibody systems with unilateral constraints. International Journal for Numerical Methods in Engineering **96**, 487–511 (2013)
15. Chung, J., Hulbert, G.: A time integration algorithm for structural dynamics with improved numerical dissipation: The generalized-α method. ASME Journal of Applied Mechanics **60**, 371–375 (1993)
16. Doyen, D., Ern, A., Piperno, S.: Time-integration schemes for the finite element dynamic Signorini problem. SIAM Journal on Scientific Computing **33**(1), 223–249 (2011)
17. Flores, P., Machado, M., Seabra, E., Tavares da Silva, M.: A parametric study on the Baumgarte stabilization method for forward dynamics of constrained multibody systems. ASME Journal of Computational and Nonlinear Dynamics **6**, 011,019–011,019–9 (2010)
18. Gear, C., Leimkuhler, B., Gupta, G.: Automatic integration of Euler-Lagrange equations with constraints. Journal of Computational and Applied Mathematics **12–13**, 77–90 (1985)
19. Géradin, M., Cardona, A.: Flexible Multibody Dynamics: A Finite Element Approach. John Wiley & Sons, Chichester (2001)
20. Haddouni, M., Acary, V., Garreau, S., Beley, J.D., Brogliato, B.: Comparison of several formulations and integration methods for the resolution of daes formulations in event-driven simulation of nonsmooth frictionless multibody dynamics. Multibody System Dynamics pp. 1–31 (2017)
21. Hilber, H., Hughes, T., Taylor, R.: Improved numerical dissipation for time integration algorithms in structural dynamics. Earthquake Engineering and Structural Dynamics **5**, 283–292 (1977)
22. Hintermüller, M., Ito, K., Kunish, K.: The primal-dual active set strategy as a semismooth Newton method. SIAM Journal on Optimization **13**(3), 865–888 (2003)
23. Hüeber, S., Stadler, G., Wohlmuth, B.I.: A primal-dual active set algorithm for three-dimensional contact problems with coulomb friction. SIAM J. Sci. Comput. **30**(2), 572–596 (2008). DOI 10.1137/060671061. URL http://dx.doi.org/10.1137/060671061
24. Hüeber, S., Wohlmuth, B.: A primaldual active set strategy for non-linear multibody contact problems. Computer Methods in Applied Mechanics and Engineering **194**(2729), 3147 – 3166 (2005). DOI http://dx.doi.org/10.1016/j.cma.2004.08.006. URL http://www.sciencedirect.com/science/article/pii/S0045782504004402
25. Jean, M.: The non-smooth contact dynamics method. Computer Methods in Applied Mechanics and Engineering **177**, 235–257 (1999)
26. Moreau, J.: Bounded variation in time. In: J. Moreau, P. Panagiotopoulos, G. Strang (eds.) Topics in Nonsmooth Mechanics, pp. 1–74. Birkhäuser, Basel (1988)
27. Moreau, J.J.: Unilateral contact and dry friction in finite freedom dynamics. In: J.J. Moreau, P. Panagiotopoulos (eds.) Non-smooth mechanics and applications, vol. 302, pp. 1–82. Springer-Verlag, Wien - New York (1988)
28. Newmark, N.: A method of computation for structural dynamics. ASCE Journal of the Engineering Mechanics Division **85**, 67–94 (1959)
29. Paoli, L., Schatzman, M.: A numerical scheme for impact problems I: The one-dimensional case. SIAM Journal of Numerical Analysis **40**, 702–733 (2002)
30. Paoli, L., Schatzman, M.: A numerical scheme for impact problems II: The multi-dimensional case. SIAM Journal of Numerical Analysis **40**, 734–768 (2002)
31. Pfeiffer, F.: On non-smooth dynamics. Meccanica **43**, 533–554 (2008)
32. Pfeiffer, F., Foerg, M., Ulbrich, H.: Numerical aspects of non-smooth multibody dynamics. Computer Methods in Applied Mechanics and Engineering **195**, 6891–6908 (2006)
33. Pfeiffer, F., Glocker, C.: Multibody dynamics with unilateral contacts. Wiley Series in Nonlinear Science. Wiley-VCH, Weinheim (2004)
34. Schindler, T., Acary, V.: Timestepping schemes for nonsmooth dynamics based on discontinuous Galerkin methods: Definition and outlook. Mathematics and Computers in Simulation **95**(Supplement C), 180–199 (2014)
35. Schindler, T., Rezaei, S., Kursawe, J., Acary, V.: Half-explicit timestepping schemes on velocity level based on time-discontinuous Galerkin methods. Computer Methods in Applied Mechanics and Engineering **290**(Supplement C), 250 – 276 (2015)

36. Schoeder, S., Ulbrich, H., Schindler, T.: Discussion on the Gear-Gupta-Leimkuhler method for impacting mechanical systems. Multibody Systems Dynamics **31**, 477–495 (2013)
37. Studer, C., Leine, R.I., Glocker, C.: Step size adjustment and extrapolation for time-stepping schemes in non-smooth dynamics. International Journal for Numerical Methods in Engineering **76**(11), 1747–1781 (2008)